Supporting Information

Rodriguez-Emmenegger et al.

1. Materials

All reagents were obtained from commercial sources and used without purification unless otherwise stated. CH_2Cl_2 (DCM) was dried over CaH_2 and freshly distilled before use. DMF was dried from CaH_2, distilled, and kept over molecular sieves prior to use. Solvents and reagents were deoxygenated when necessary by purging with nitrogen. Milli-Q water obtained by Milli-Q UV plus with the resistivity 18.2 MΩ·cm was used for the preparation of phosphate-buffered saline (PBS). PBS (1×) was obtained by dissolving 8 g of NaCl, 0.2 g of KCl, 1.44 g of Na_2HPO_4 and 0.24 g of KH_2PO_4 in 800 mL of Milli-Q water, adjusted to pH = 7.4 and diluted to 1,000 mL. The wild-type galectins were obtained by recombinant production and purification by affinity chromatography as crucial step, in each case rigorously checked for purity by one- and two-dimensional gel electrophoresis, mass spectrometry including peptide fingerprinting and gel filtration. Quaternary structure was also assessed by ultracentrifugation. Haemagglutination assays served as activity control. Respective protocols have been reported previously for Gal-1 (1), Gal-8S (2), and $(Gal\text{-}1)_4$–GG (3). No unexpected or unusually high safety hazards were encountered.

2. Techniques

^1H and ^{13}C NMR spectra were recorded at 500 MHz and 126 MHz respectively, on a Bruker DRX (500 MHz) NMR spectrometer. All NMR spectra were measured at 23 °C in $CDCl_3$. Chemical shifts (δ) are reported in ppm and coupling constants (J) are reported in Hertz (Hz). The resonance multiplicities in the ^1H NMR spectra are described as “s” (singlet), “d” (doublet), “t” (triplet), “quint” (quintet) and “m” (multiplet) and broad resonances are indicated by “br”. Residual protic solvent of $CDCl_3$ (^1H, δ 7.26 ppm; ^{13}C, δ 77.16 ppm), or DMSO-d_6 (^1H, δ 2.50 ppm; ^{13}C, δ 39.52 ppm), and tetramethylsilane (TMS, δ 0 ppm) were used as the internal reference in the ^1H- and ^{13}C-NMR spectra. The absorptions are given in wavenumbers (cm^{-1}). Evolution of the reaction was monitored by thin-layer chromatography (TLC) using silica gel 60 F_{254} precoated plates (E. Merck) and compounds were visualized by UV light with a wavelength of 254 or 356 nm. Purifications by flash column chromatography were performed using flash silica gel from Silicycle (60 Å, 40–63 μm) with the indicated eluent. The purity of the products was determined by a combination of TLC and high-pressure liquid chromatography (HPLC) was carried out

www.pnas.org/cgi/doi/10.1073/pnas.1821924116

using Shimadzu LC-20AD high-performance liquid chromatograph pump, a PE Nelson Analytical 900 Series integration data station, a Shimadzu RID-10A refractive index (RI) detector, a Shimadzu SPD-10A VP (UV-*vis*, λ = 254 nm) and three AM gel columns (a guard column, two 500 Å, 10 μm columns). THF was used as solvent at the oven temperature of 23 ºC. Detection was done by UV absorbance at 254 nm. MALDI-TOF mass spectrometry was performed on a PerSeptive Biosystem-Voyager-DE (Framingham, MA) mass spectrometer equipped with nitrogen laser (337 nm) and operating in linear mode. Internal calibration was performed using Angiotensin II and Bombesin as standards. The analytical sample was obtained by mixing the THF solution of the sample (5–10 mg/mL) and THF solution of the matrix (2,5-dihydroxybenzoic acid, 10 mg/mL) in a 1/5 (v/v) ratio. The prepared solution of the sample and the matrix (0.5 μL) was loaded on the MALDI plate and allowed to dry at 23 ºC before the plate was inserted into the vacuum chamber of the MALDI instrument. The laser steps and voltages applied were adjusted depending on both the molecular weight and the nature of each analyzed compound. Elemental analysis was performed by M-H-W Laboratories (Phoenix, AZ).

3. Synthesis

2,2-bis(3,5-didodecyloxybenzonate)propionic acid (**1**) (4), (2-phenyl-1,3-dioxane-5,5-diyl)dimethanol (**2**) (5), 2-methyl-3-(prop-2-yn-1-yloxy)-2-((prop-2-yn-1-yloxy)methyl)propanoic acid (**5**) (6), 2-[2-(2-Azidoethoxy)ethoxy]ethyl 4-O-β-D-galactopyranosyl-β-D-glucopyranoside (**7**) (7), Compond **8** (4), 3,4,5-tris{2-[2-(2-methoxyethoxy)ethoxy]ethoxy}benzoic acid (**9**) (5), 3,5-bis(dodecyloxy)benzoic acid **(12)** (5), Compond **14** (4), single-single Janus glycodendrimer **JGD-1$_{Lac}$** (8), twin-twin Janus glycodendrimer **JGD-2$_{Lac}$** (8), twin-mixed Janus glycodendrimer **JGD(3/1$_{Lac}$)** (8), sequence-defined Janus glycodendrimers **JGD(6/1$_{Lac}$)** (4), **JGD(8/1$_{Lac}^{2S}$)** (4), **JGD(8/1$_{Lac}^{3S}$)** (4), **JGD(8/1$_{Lac}^{2L}$)** (4), and **JGD(8/1$_{Lac}^{3L}$)** (4) were prepared according to literature procedures.

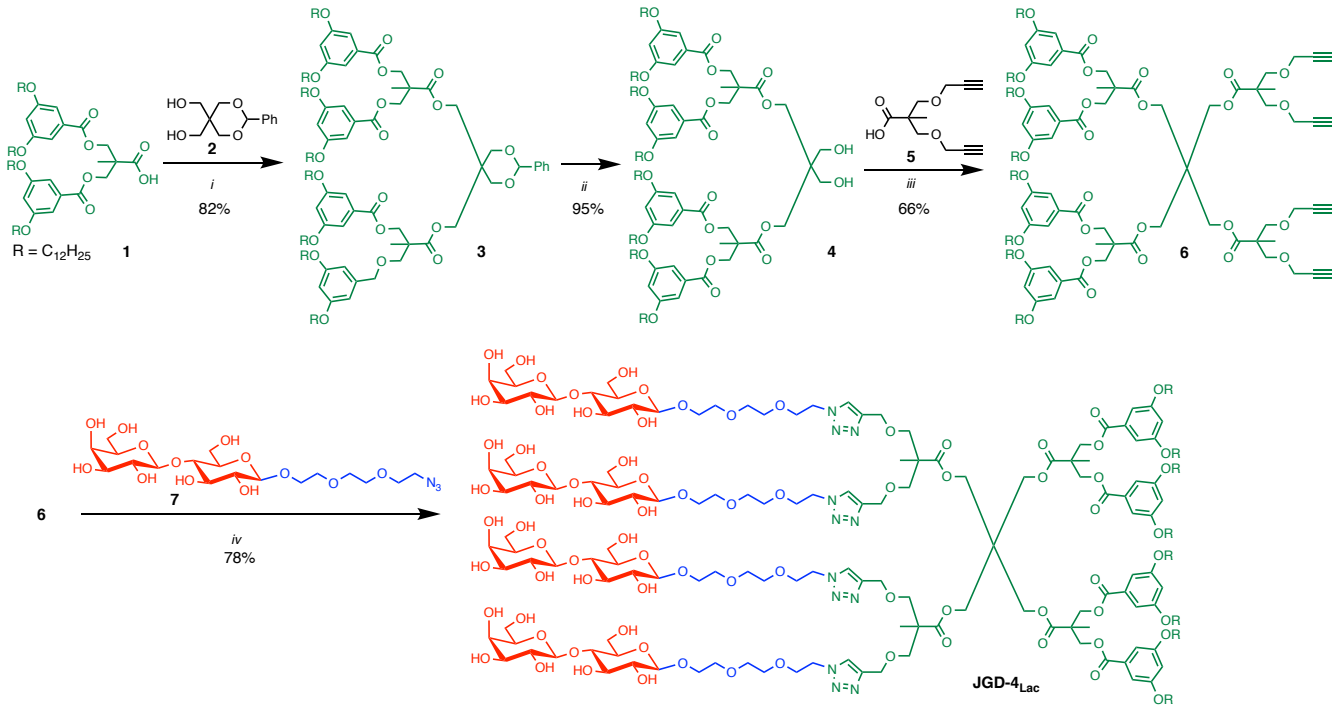

Fig. S1. Synthesis of JGD-4. Reagents and conditions: (*i*) DPTS, DCC, DCM, 23 °C; (*ii*) 10% Pd/C, H_2, DCM, MeOH, 23 °C; (*iii*) DPTS, DCC, DCM, 23 °C; (*iv*) $CuSO_4 \cdot 5H_2O$, sodium ascorbate, DMF, H_2O, 23 °C.

Synthesis of Compound ***3***. To a DCM (10 mL) solution of compound **1** (1.50 g, 1.39 mmol), compound **2** (141 mg, 0.63 mmol) and 4-(dimethylamino)pyridinium 4-toluenesulfonate (DPTS) (9) (409 mg, 1.39 mmol), was added *N*,*N*'-dicyclohexylcarbodiimide (DCC) (520 mg, 2.52 mmol). The mixture was allowed to stir at 23 ºC for 24 h. The precipitate was filtered, and the filtrate was concentrated to dryness. The crude product was further purified by column chromatography with a mobile phase of hexane/DCM = 1/1 to 1/2 (v/v) to yield compound **3** as a colorless oily liquid (1.08 g, 73%). ^{1}H NMR (500 MHz, $CDCl_3$) δ = 7.29 (m, 5H, 5×Ph*H*), 7.09 (d, 8H, J = 2.2 Hz, 8×Ph*H*), 6.60–6.61 (t, 4H, J = 2.2 Hz, 4×Ph*H*), 5.20 (s, 1H, Ph-C*H*(OCH_2-)$_2$), 4.47–4.61 (m, 10H, 10×C*H*HO), 4.02–4.04 (d, 2H, J = 12 Hz, 2×C*H*HO), 3.98 (s, 2H, 2×C*H*HO), 3.90–3.92 (t, 16H, J = 6.8 Hz, 8×O*CH*$_2$$CH_2CH_2(CH_2)_8CH_3$), 3.76–3.79 (d, 2H, J = 12 Hz, 2×C*H*HO), 1.70–1.77 (m, 16H, 8×OCH_2*CH*$_2$$CH_2(CH_2)_8CH_3$), 1.39–1.46 (m, 22H, 8×$OCH_2CH_2$*CH*$_2$$(CH_2)_8CH_3$ and 2×CH_3), 1.26–1.30 (m, 128H, 8×$OCH_2CH_2CH_2$(*CH*$_2$$)_8CH_3$), 0.87–0.90 (m, 24H, 8×$OCH_2CH_2CH_2(CH_2)_8$*CH*$_3$). ^{13}C NMR (126 MHz, $CDCl_3$) δ = 172.28, 172.23, 165.86, 165.83, 160.37, 160.31, 137.64, 131.31, 131.25, 128.98, 128.19, 126.09, 107.82, 107.78, 106.76, 106.67, 101.93,

69.24, 68.41, 68.38, 65.93, 63.82, 63.40, 47.13, 47.11, 37.80, 32.03, 29.79, 29.76, 29.74, 29.70, 29.53, 29.47, 29.30, 26.14, 22.79, 18.23, 28.14, 14.20.

*Synthesis of Compound **4***. To a mixed DCM (50 mL) and MeOH (25 mL) solution of compound **3** (1.08 g, 0.46 mmol) was added palladium on carbon (10% Pd/C, 100 mg). The mixture was bubbled with H_2 for 30 min and then allowed to stir at 23 ºC for 12 h under H_2 atmosphere. The mixture was then filtered through Celite®. The filtrate was concentrated to dryness under reduced pressure to yield compound **4** as an oily liquid (0.99 g, 95%). ^{1}H NMR (500 MHz, $CDCl_3$) δ = 7.09 (d, 8H, J = 2.2 Hz, 8×Ph*H*), 6.62 (t, 4H, J = 2.2 Hz, 4×Ph*H*), 4.57–4.59 (d, 4H, J = 11.5 Hz, 4×C*H*HO), 4.49–4.51 (d, 4H, J = 11.5 Hz, 4×C*H*HO), 4.20 (s, 4H, 2×CH_2), 3.92–3.95 (t, 16H, J = 6.5 Hz, 8×OC*H*$_2$CH$_2$CH$_2$(CH$_2$)$_8$CH$_3$), 3.59–3.60 (d, 4H, J = 6 Hz, 2×C*H*$_2$OH), 2.68–2.71 (t, 2H, J = 6 Hz, 2×CH$_2$O*H*), 1.72–1.78 (m, 16H, 8×OCH$_2$C*H*$_2$CH$_2$(CH$_2$)$_8$CH$_3$), 1.39–1.45 (m, 16H, 8×OCH$_2$CH$_2$C*H*$_2$(CH$_2$)$_8$CH$_3$), 1.26–1.30 (m, 134H, 8×OCH$_2$CH$_2$CH$_2$(C*H*$_2$)$_8$CH$_3$ and 2×CH$_3$), 0.86–0.89 (m, 24H, 8×OCH$_2$CH$_2$CH$_2$(CH$_2$)$_8$C*H*$_3$). ^{13}C NMR (126 MHz, $CDCl_3$) δ = 173.00, 165.96, 160.32, 131.22, 107.90, 106.67, 68.47, 66.06, 63.26, 61.85, 47.27, 45.29, 32.04, 29.80, 29.76, 29.74, 29.71, 29.53, 29.48, 29.30, 26.14, 22.80, 18.10, 14.21.

*Synthesis of Compound **6***. To a DCM (10 mL) solution of compound **4** (0.99 g, 0.44 mmol), compound **5** (368 mg, 1.75 mmol) and DPTS (515 mg, 1.75 mmol), was added DCC (722 mg, 3.5 mmol). The mixture was allowed to stir at 23 ºC for 24 h. The precipitate was filtered, and the filtrate was concentrated to dryness. The crude product was further purified by column chromatography with a mobile phase of hexane/DCM = 7/1 to yield compound **6** as an oily liquid (0.77 g, 66%). Purity (HPLC): 99%+. ^{1}H NMR (500 MHz, $CDCl_3$) δ = 7.08 (d, 8H, J = 2.2 Hz, 8×Ph*H*), 6.60 (t, 4H, J = 2.2 Hz, 4×Ph*H*), 4.60–4.62 (d, 4H, J = 11.5 Hz, 4×C*H*HO), 4.45–4.47 (d, 4H, J = 11.5 Hz, 4×C*H*HO), 4.20 (s, 4H, 2×CH_2), 4.17 (s, 4H, 2×CH_2), 4.06 (s, 8H, 4×CH_2), 3.91–3.94 (t, 16H, J = 6.5 Hz, 8×OC*H*$_2$CH$_2$CH$_2$(CH$_2$)$_8$CH$_3$), 3.51 (s, 8H, 4×OC*H*$_2$CCH), 2.41–2.42 (t, 4H, J = 2.3 Hz, OCH$_2$CC*H*), 1.72–1.78 (m, 16H, 8×OCH$_2$C*H*$_2$CH$_2$(CH$_2$)$_8$CH$_3$), 1.38–1.46 (m, 16H, 8×OCH$_2$CH$_2$C*H*$_2$(CH$_2$)$_8$CH$_3$), 1.26–1.32 (m, 134H, 8×OCH$_2$CH$_2$CH$_2$(C*H*$_2$)$_8$CH$_3$ and 2×CH$_3$), 1.11 (s, 6H, 2×CH$_3$), 0.86–0.89 (m, 24H, 8×OCH$_2$CH$_2$CH$_2$(CH$_2$)$_8$C*H*$_3$). ^{13}C NMR (126 MHz, $CDCl_3$) δ = 173.14, 171.96, 165.96, 160.31, 131.44, 107.9, 106.6, 79.62, 74.86, 71.71, 68.43, 65.73, 62.61, 61.35, 58.62, 48.21, 46.96, 43.44, 32.05, 29.81, 29.77, 29.76, 29.72, 29.56, 29.48, 29.34, 26.17, 22.81, 18.15, 17.88, 14.23. MALDI-TOF (m/z): $[M+K]^+$ calcd for $C_{161}H_{260}KO_{28}$, 2682.9; found 2683.9.

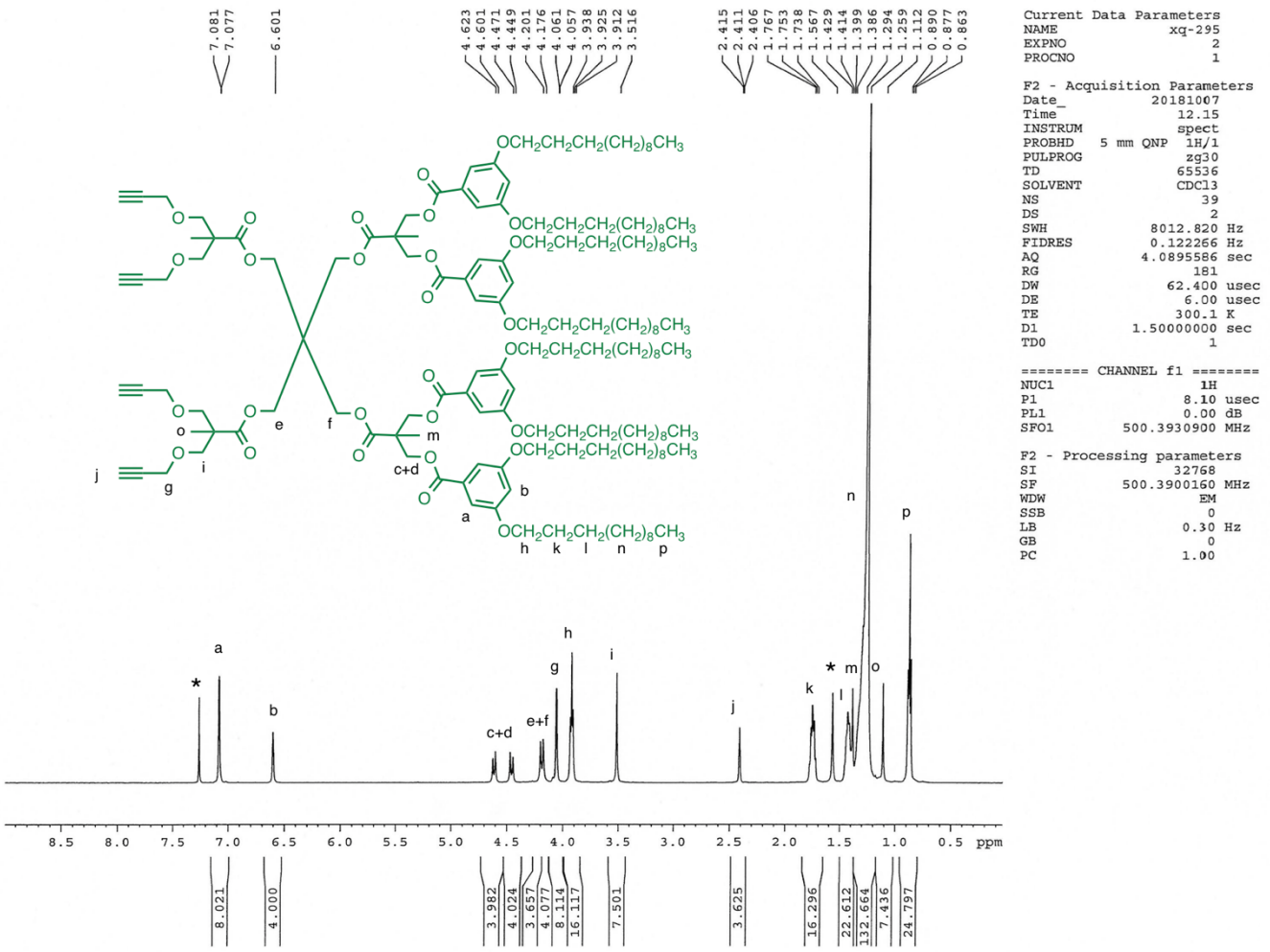

Fig. S2. The ^{1}H NMR spectrum of compound **6** ($CDCl_3$, 500 MHz). Asterisked signals at δ 7.26 ppm and 1.58 ppm are due to partially nondeuterated residues of $CDCl_3$ and water, respectively.

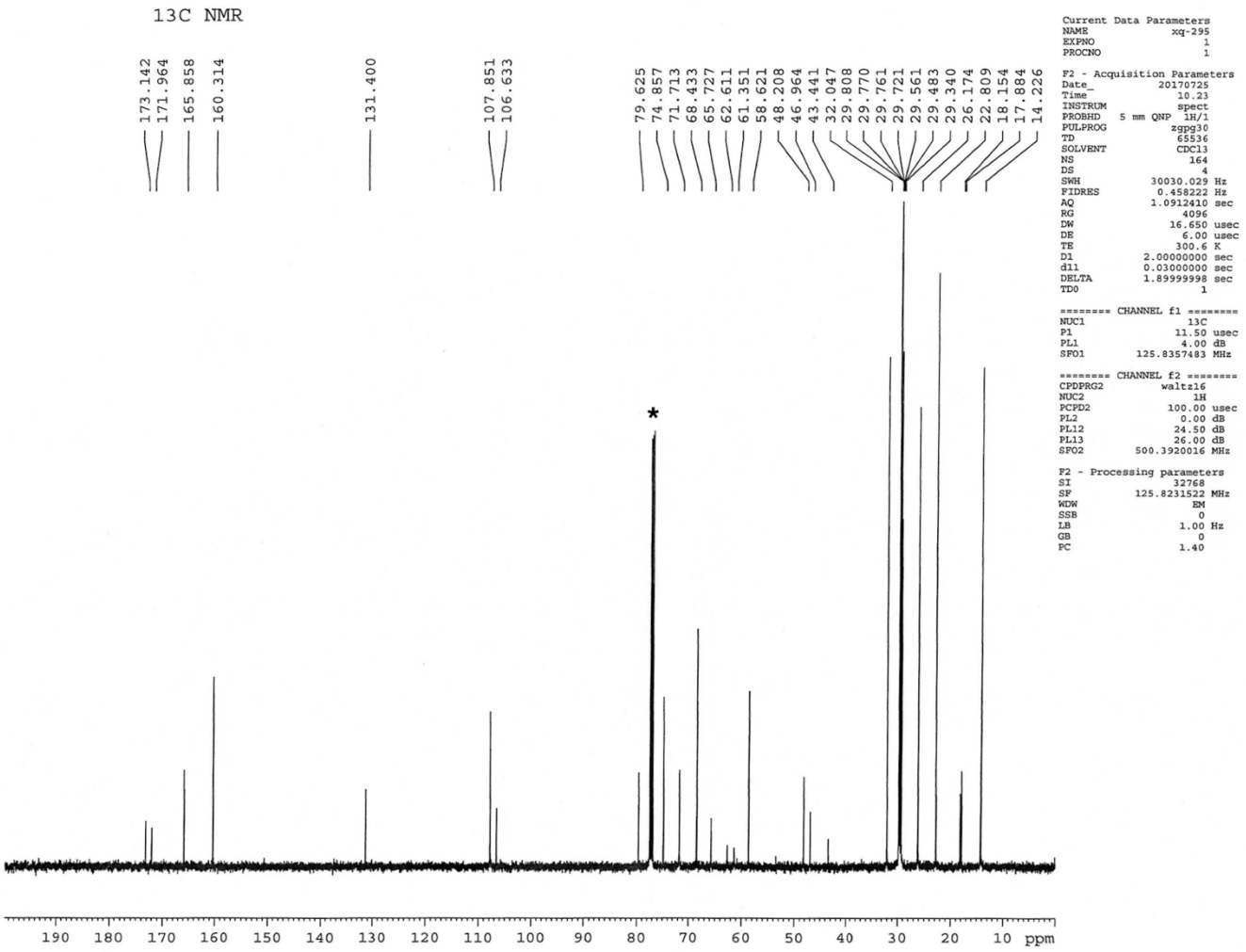

Fig. S3. The ^{13}C NMR spectrum of compound **6** ($CDCl_3$, 126 MHz). Asterisked signal at δ 77.16 ppm is due to $CDCl_3$.

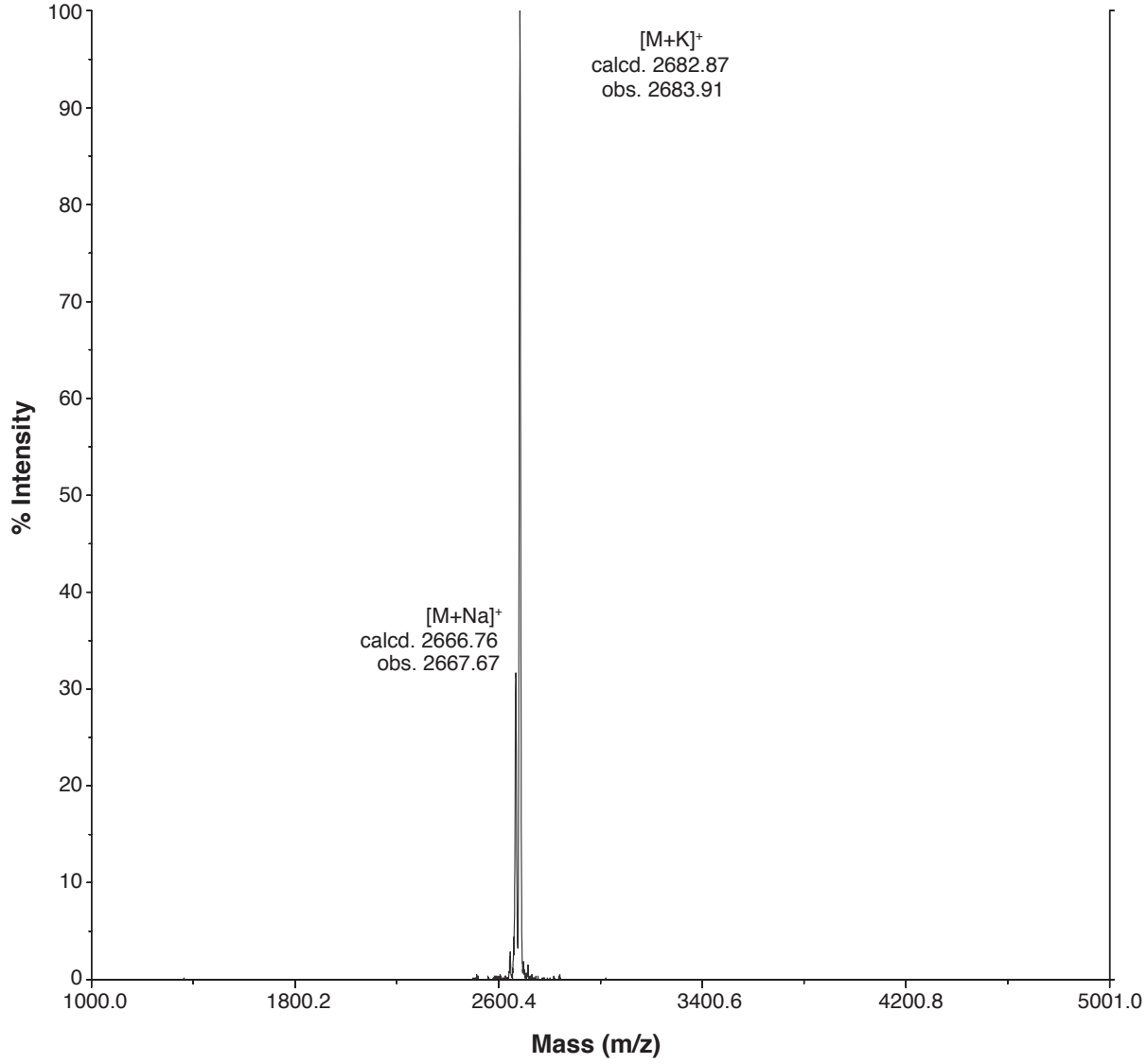

Fig. S4. MALDI-TOF mass spectrum of compound **6**.

*Synthesis of **JGD-4***. To a mixed solution of compound **6** (230 mg, 0.087 mmol) and **7** (219 mg, 0.44 mmol) in DMF (10 mL), was added $CuSO_4 \cdot 5H_2O$ (110 mg, 0.44 mmol) in water (1 mL), and sodium ascorbate (174 mg, 0.88 mmol) in water (1 mL) successively under nitrogen atmosphere. The reaction mixture was allowed to stir at 23 ºC for 24 h. The reaction mixture was concentrated to dryness under reduced pressure. The crude product was stirred with NH_3/NH_4Cl buffer (pH = 10) for 30 min to remove the copper ions and then extracted with DCM. The DCM solution was dried by Na_2SO_4 and was further purified by Sephadex® LH-20 (Sigma-Aldrich) gel filtration chromatography (in 1 $cm^2 \times 40$ cm column) with a mobile phase of $CHCl_3$/MeOH (1/1, v/v) to yield **JGD-4** as white solid (316 mg, 78%). Purity (HPLC): 99%+. ^{1}H NMR (500 MHz, DMSO-d_6) δ = 7.96 (s, 4H, 4×triazole-H), 7.08 (s, 8H, 8×Ph*H*), 6.60

(s, 4H, 4×Ph*H*), 5.09–5.10 (d, 4H, J = 5 Hz), 5.07–5.08 (d, 4H, J = 4 Hz), 4.75–4.76 (d, 4H, J = 5 Hz), 4.67 (s, 4H), 4.62–4.64 (m, 6H), 4.53–4.56 (m, 6H), 4.47–4.50 (m, 16H), 4.43 (m, 8H), 4.20–4.22 (m, 10H), 3.72–3.85 (m, 36H), 3.62 (m, 10H), 3.47–3.58 (m, 56H), 3.25–3.30 (m, 20H), 3.00–3.02 (m, 4H), 1.53 (m, 16H, 8×$OCH_2CH_2CH_2(CH_2)_8CH_3$), 1.24 (m, 24H, 8×$OCH_2CH_2CH_2(CH_2)_8CH_3$ and 2×CH_3), 1.11 (m, 128H, 8×$OCH_2CH_2CH_2(CH_2)_8CH_3$), 1.00 (s, 6H, 2×$CH_3$), 0.73–0.75 (m, 24H, 8×$OCH_2CH_2CH_2(CH_2)_8CH_3$). ^{13}C NMR (126 MHz, DMSO-d_6) δ = 172.84, 171.45, 164.66, 159.51, 143.48, 131.00, 124.03, 106.85, 105.72, 103.83, 102.66, 80.70, 75.49, 74.97, 74.80, 73.23, 73.08, 71.63, 71.28, 70.57, 69.62, 69.49, 68.69, 68.14, 67.99, 67.34, 63.97, 60.51, 60.40, 49.26, 47.86, 46.16, 31.38, 29.20, 29.15, 28.92, 28.86, 28.61, 25.51, 22.10, 17.56, 17.40, 13.53. MALDI-TOF (m/z): $[M+K]^+$ calcd for $C_{233}H_{392}N_{12}KO_{80}$, 4677.4; found 4675.1. Elemental Analysis calcd for $C_{233}H_{392}N_{12}O_{80}$, C, 60.29; H, 8.51; N, 3.57 found: C, 60.12; H, 8.50; N, 3.44.

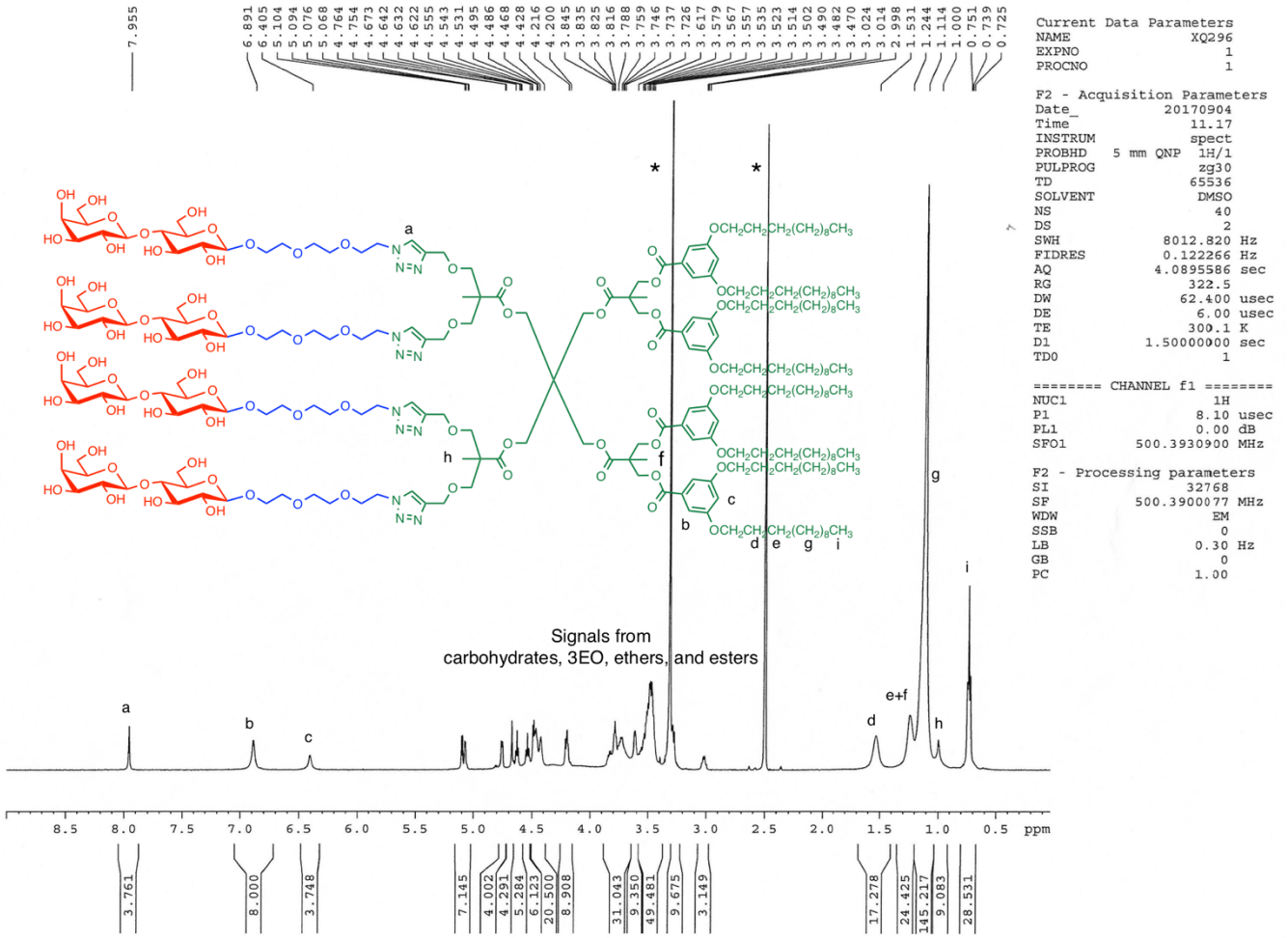

Fig. S5. The ^{1}H NMR spectrum of **JGD-4$_{Lac}$** (DMSO-d_6, 500 MHz). Asterisked signals at δ 2.50 ppm and 3.33 ppm are due to partially nondeuterated residues of DMSO-d_6 and water, respectively.

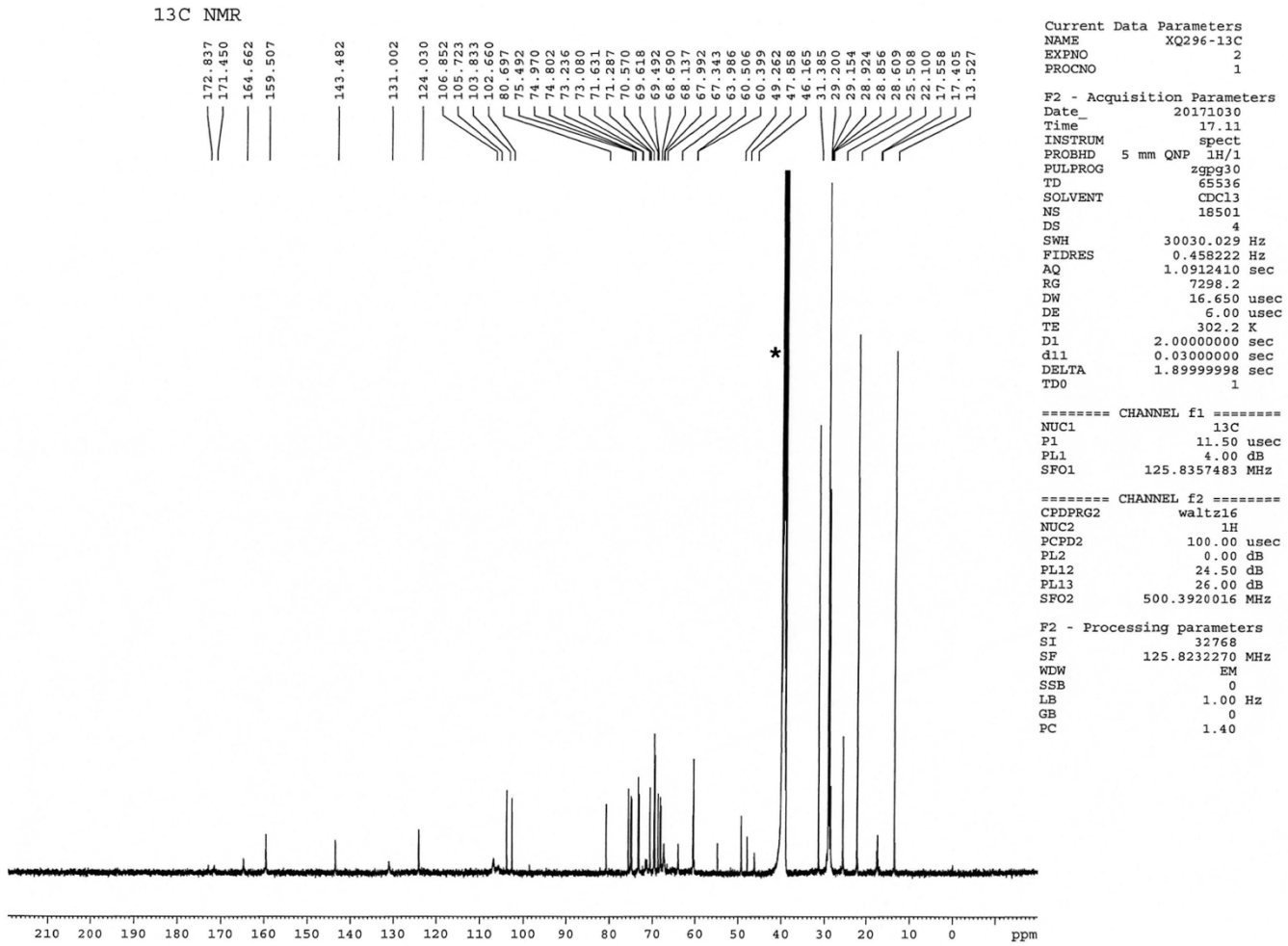

Fig. S6. The ^{13}C NMR spectrum of **JGD-4$_{Lac}$** (DMSO-d_6, 126 MHz). Asterisked signal at δ 39.52 ppm is due to DMSO-d_6.

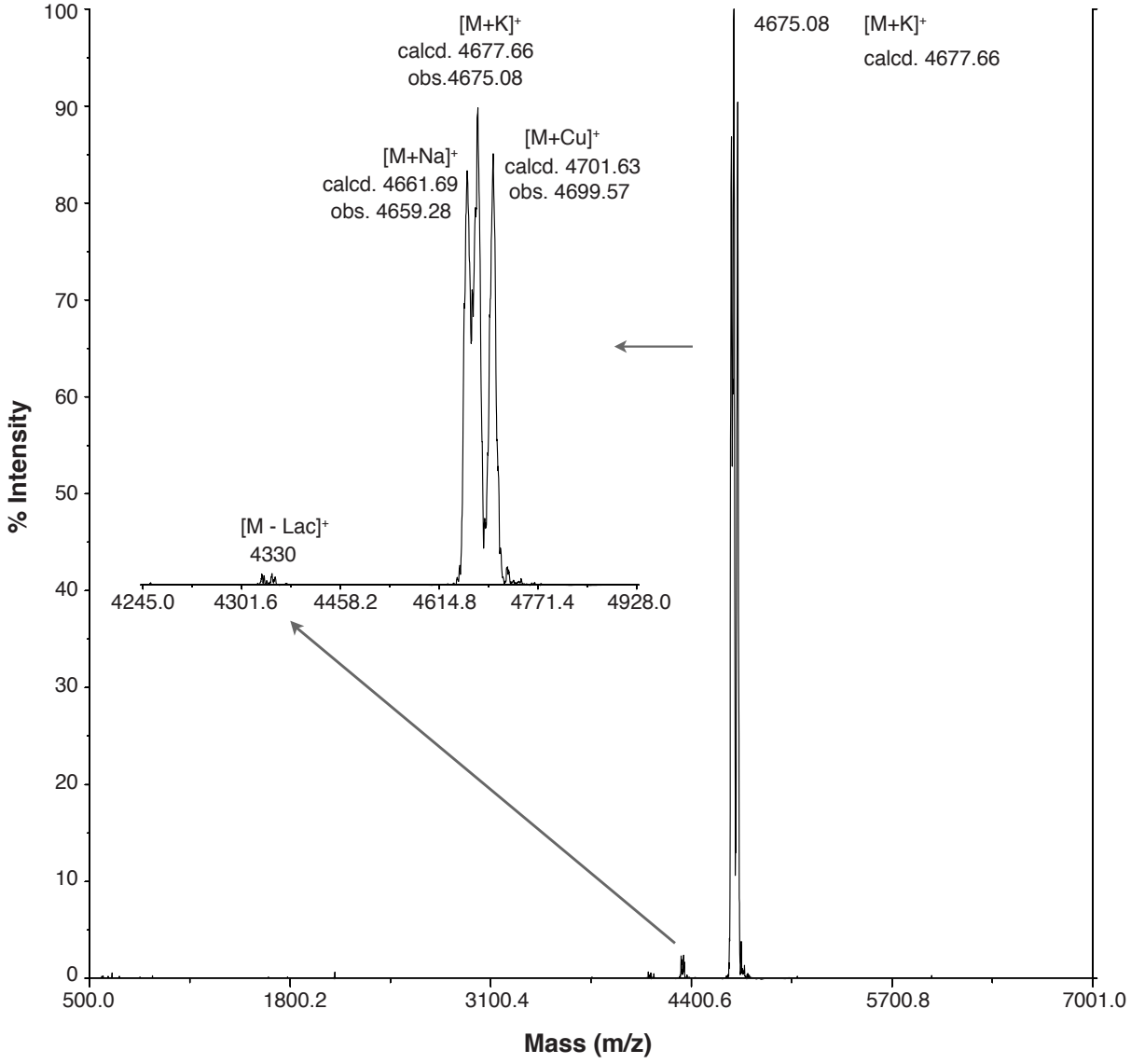

Fig. S7. MALDI-TOF mass spectrum of **JGD-4$_{Lac}$**. Inset panel shows an expanded portion of the spectrum. The very small peaks around m/z = 4330 arise from the fragment missing one Lac $[M - Lac]^+$ generated by MALDI cleavage. $[M+Cu]^+$ is produced during the click reaction step.

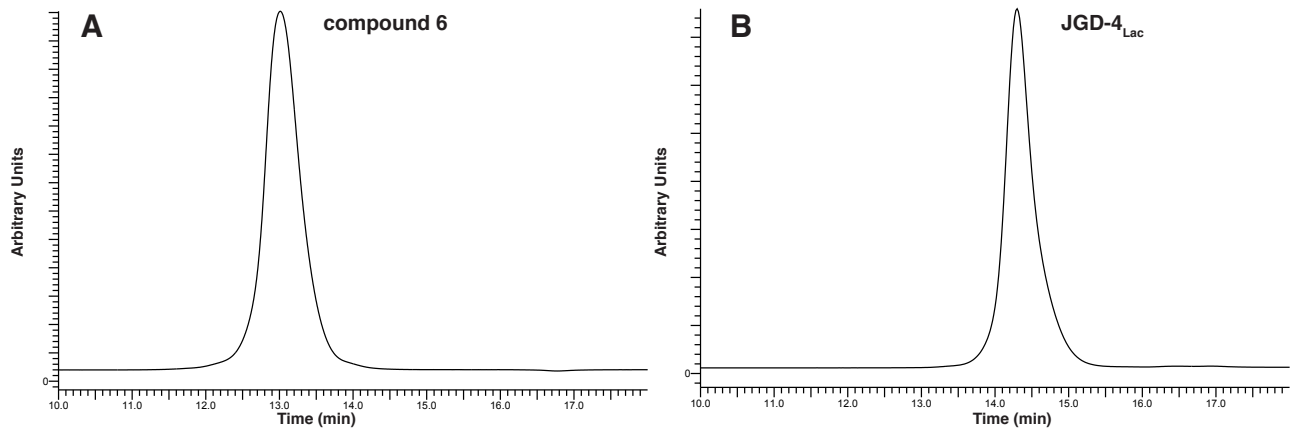

Fig. S8. HPLC traces. **A**, HPLC trace of compound **6**; **B**, HPLC trace of **JGD-4$_{Lac}$**. UV-*vis* detector was set at $\lambda = 254$ nm.

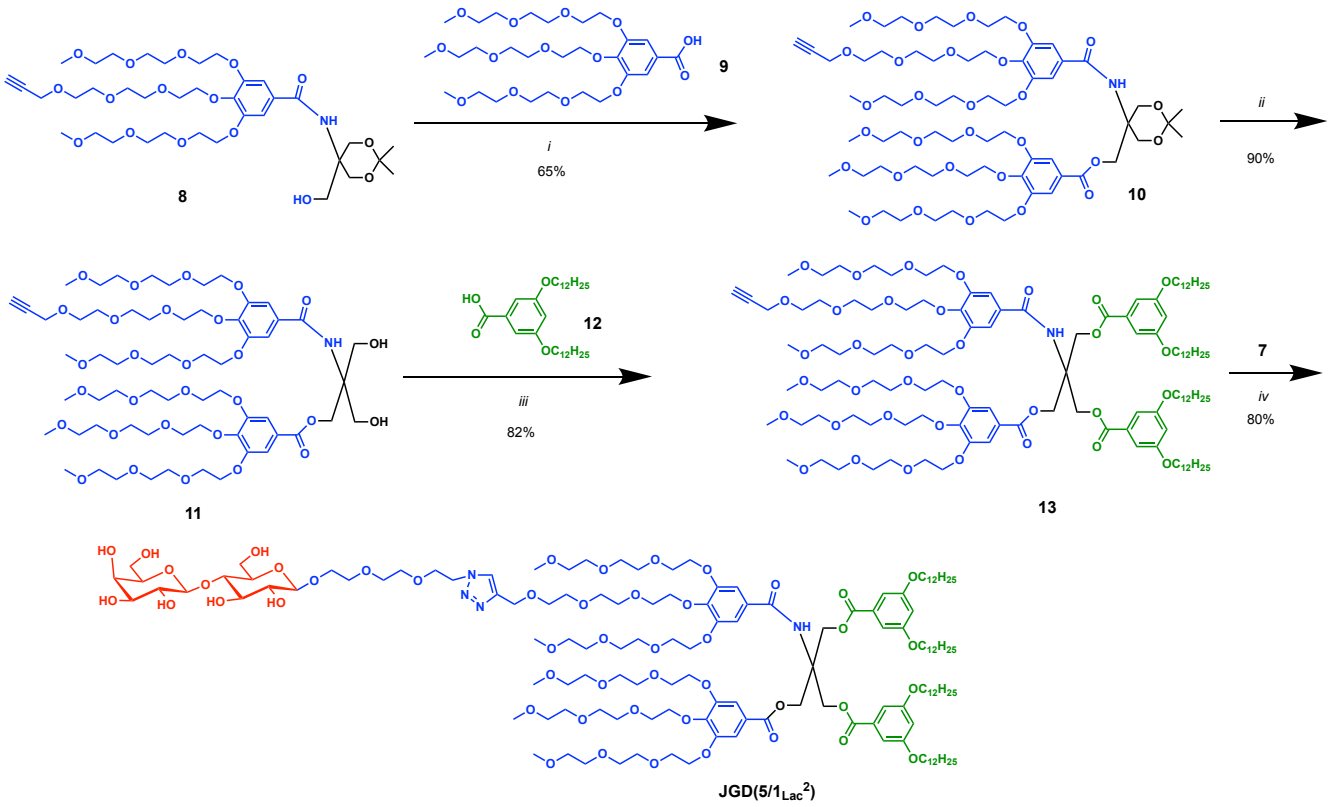

Fig. S9. Synthesis of JGD(5/1$_{Lac}^2$). *Reagents and conditions*: (*i*) DPTS, DCC, DCM, 23 °C; (*ii*) MeOH, HCl (2M, aq), 23 °C; (*iii*) DPTS, DCC, DCM, 23 °C; (*iv*) $CuSO_4 \cdot 5H_2O$, sodium ascorbate, THF, H_2O, 23 °C.

*Synthesis of Compound **10***. To a DCM (10 mL) solution of compound **8** (987 mg, 1.27 mmol), compound **9** (771 mg, 1.27 mmol) and DPTS (374 mg, 1.27 mmol), was added DCC (524 mg, 2.54 mmol). The mixture was allowed to stir at 23 ºC for 24 h. The precipitate was filtered, and the filtrate was concentrated to dryness. The crude product was further purified by column chromatography with a mobile phase of DCM/methanol = 40/1 (v/v) to yield compound **10** as a colorless oily liquid (1.12 g, 65%). ^{1}H NMR (500 MHz, $CDCl_3$) δ = 7.30 (s, 2H, 2×Ph*H*), 7.14 (s, 1H, -N*H*), 7.05 (s, 2H, 2×Ph*H*), 4.81 (s, 2H, -COOCH_2), 4.62 (d, 2H, J = 11.9 Hz, -OCH_2), 4.15-4.23 (m, 16H, 6×(PhOCH_2CH_2O-) and -OCH_2CCH and -OCH_2), 3.70-3.71 (m, 12H, 6×(PhOCH$_2$CH_2O-)), 3.62-3.65 (m, 24H, 6×(PhOCH$_2$CH$_2$OCH_2CH_2O-)), 3.51-3.53 (m, 12H, 6×(PhOCH$_2$CH$_2$OCH$_2$CH$_2$OCH_2CH$_2$-)), 3.47 (m, 12H, 6×(PhOCH$_2$CH$_2$OCH$_2$CH$_2$OCH$_2$CH_2-)), 3.35 (m, 15H, 5×(-OCH_3)), 2.44 (t, 1H, J = 2.2Hz, -CC*H*), 1.60 (s, 3H, -OCCH_3), 1.47 (s, 3H, -OCCH_3). ^{13}C NMR (126 MHz, $CDCl_3$) δ = 167.31, 167.03, 152.43, 143.30, 141.42, 129.39, 124.05, 109.44, 106.75, 98.74, 79.68, 74.66, 72.48, 72.41, 71.92, 70.78, 70.75, 70.65, 70.55, 70.52, 70.50, 70.39, 69.64, 69.61, 69.11, 69.04, 68.93, 64.92, 61.62, 59.00, 58.38, 53.98, 50.63, 25.29, 22.27.

*Synthesis of Compound **11***. To a methanol solution (20 mL) of compound **10** (1120 mg, 0.82 mmol), were added 2 mL of HCl aqueous solution (2M). The mixture was stirred at 23 ºC for 2h and water was added. Then, the mixture was extracted with DCM for 3 times. An organic extract was dried over Na_2SO_4, and evaporated to dryness under reduced pressure to yield compound **10** as a colorless viscous liquid (975 mg, 90%). ^{1}H NMR (500 MHz, $CDCl_3$) δ = 7.31 (s, 2H, 2×Ph*H*), 7.22 (s, 1H, -NH), 7.09 (s, 2H, 2×Ph*H*), 4.63 (s, 2H, -COOCH_2), 4.51 (s, 2H, 2×-CH$_2$O*H*), 4.17-4.23 (m, 18H, 6×(-PhOCH_2CH$_2$O-) and -OCH_2CCH and 2×(-CH_2OH)), 3.83-3.86 (m, 12H, 6×(PhOCH$_2$CH_2O-)), 3.69-3.72 (m, 12H, 6×(PhOCH$_2$CH$_2$OCH_2CH$_2$O-)), 3.62-3.66 (m, 24H, 6×(PhOCH$_2$CH$_2$OCH$_2$CH_2OCH_2CH$_2$-)), 3.51-3.54 (m, 12H, 6×(PhOCH$_2$CH$_2$OCH$_2$CH_2OCH$_2$CH_2-)), 3.35-3.36 (m, 15H, 5×(-OCH_3)), 2.44 (t, 1H, J = 2.2Hz, -CCH). ^{13}C NMR (126 MHz, $CDCl_3$) δ = 168.13, 166.60, 152.42, 152.31, 143.07, 141.71, 129.07, 124.17, 109.38, 107.34, 79.61, 74.66, 72.39, 72.35, 71.86, 71.84, 71.82, 70.70, 70.61, 70.59, 70.58, 70.52, 70.49, 70.44, 70.35, 70.32, 69.65, 69.56, 69.08, 69.03, 68.94, 63.20, 63.13, 61.90, 58.93, 58.31.

*Synthesis of Compound **13***. To a DCM (10 mL) solution of compound **11** (440 mg, 0.33 mmol), compound **12** (328 mg, 0.67 mmol) and DPTS (197 mg, 0.67 mmol), was added DCC (276 mg, 1.34 mmol). The mixture was allowed to stir at 23 ºC for 24 h. The precipitate was filtered, and the filtrate was concentrated

to dryness. The crude product was further purified by column chromatography with a mobile phase of DCM/methanol = 30/1 (v/v) to yield compound **13** as a colorless oily liquid (621 mg, 82%). ^{1}H NMR (500 MHz, $CDCl_3$) δ = 7.41 (s, 1H, -NH), 7.24 (s, 2H, 2×Ph*H*), 7.08 (d, 4H, J = 2.5Hz, 4×Ph*H*), 7.04 (s, 2H, 2×Ph*H*), 6.60 (t, 2H, J = 2.2Hz, 2×Ph*H*), 4.92-4.99 (m, 6H, 3×(-COOCH_2)), 4.16-4.21 (m, 12H, 6×(-PhOCH_2CH_2O-)), 4.09-4.11 (m, 2H, -OCH_2CCH), 3.88 (t, 8H, J = 6.5Hz, 4×(PhOCH_2-)), 3.77-3.85 (m, 12H, 6×(PhOCH$_2$CH_2O-)), 3.69-3.71 (m, 12H, 6×(PhOCH$_2$CH$_2$OCH_2CH$_2$O-)), 3.60-3.65 (m, 24H, 6×(PhOCH$_2$CH$_2$OCH$_2$CH_2OCH_2CH$_2$-)), 3.50-3.54 (m, 12H, 6×(PhOCH$_2$CH$_2$OCH$_2$CH$_2$OCH$_2$CH_2-)), 3.34-3.36 (m, 15H, 5×(-OCH_3)), 2.43 (t, 1H, J = 2.2Hz, -CCH), 1.71-1.76 (m, 8H, 4×(PhOCH$_2$CH_2-)), 1.39-1.43 (m, 8H, 4×(PhOCH$_2$CH$_2$CH_2-)), 1.25-1.29 (m, 64H, 4×(PhOCH$_2$CH$_2$CH$_2$(CH_2)$_8$-)), 0.86-0.88 (m, 12H, 4×(-CH_3)). ^{13}C NMR (126 MHz, $CDCl_3$) δ = 166.89, 166.31, 166.03, 160.07, 152.37, 152.22, 142.99, 141.28, 130.76, 128.82, 123.79, 109.03, 107.63, 106.58, 106.31, 79.55, 74.54, 72.30, 71.78, 70.64, 70.52, 70.38, 70.25, 69.48, 68.96, 68.76, 68.69, 68.14, 63.94, 59.82, 58.79, 58.20, 31.77, 29.53, 29.50, 29.46, 29.28, 29.21, 29.04, 25.91, 22.54, 13.98.

Synthesis of Compound ***JGD(5/1$_{Lac}^{2}$)***. To a mixed solution of compound **13** (222 mg, 0.10 mmol) in THF (10 mL) and **7** (50 mg, 0.10 mmol) in water (1 mL) was added $CuSO_4 \cdot 5H_2O$ (26 mg, 0.10 mmol) in water (1 mL), and sodium ascorbate (40 mg, 0.20 mmol) in water (1 mL), successively, under nitrogen atmosphere. The reaction mixture was allowed to stir at 23 °C for 24 h. The reaction mixture was concentrated to dryness. The crude product was further purified by silica column chromatography with a mobile phase of DCM/methanol = 5/1 (v/v) to yield **JGD(5/1$_{Lac}^{3}$)** as a colorless gel (217 mg, 80%). Purity (HPLC): 99%+. ^{1}H NMR (500 MHz, $CDCl_3$) δ = 7.91 (s, 1H, -N*H*), 7.50 (s, 1H, -CC*H*N-), 7.24 (s, 2H, 2×Ph*H*), 7.08 (s, 4H, 4×Ph*H*), 7.05 (s, 2H, 2×Ph*H*), 6.60 (s, 2H, 2×Ph*H*), 4.93-5.00 (m, 7H, 3×(-COOCH_2-) and -OC*H*O-), 4.67 (s, 2H, 2×(-O*H*)), 4.55 (s, 2H, 2×(-O*H*)), 4.42 (s, 1H, -O*H*), 4.37 (s, 1H, -OC*H*O-), 4.10-4.21 (m, 16H, 6×(-PhOCH_2CH_2O-) and -NCH_2CH_2O-), 3.94 (m, 2H, 2×(-CH$_2$O*H*)), 3.87-3.90 (m, 12H, 4×(PhOCH_2-) and -NCH$_2$CH$_2$OCH_2CH_2O-), 3.76-3.83 (m, 16H, 6×(PhOCH$_2$CH_2O-) and -NCH$_2$CH$_2$OCH$_2$CH$_2$OCH_2CH_2O-), 3.60-3.70 (m, 48H, 6×(PhOCH$_2$CH$_2$OCH_2CH_2OCH_2CH_2-)), 3.50-3.54 (m, 12H, 6×(PhOCH$_2$CH$_2$OCH$_2$CH$_2$OCH$_2$CH_2-)), 3.33-3.36 (m, 15H, 5×(-OCH_3)), 1.71-1.76 (m, 8H, 4×(PhOCH$_2$CH_2-)), 1.39-1.43 (m, 8H, 4×(PhOCH$_2$CH$_2$CH_2-)), 1.25-1.29 (m, 64H, 4×(PhOCH$_2$CH$_2$CH$_2$(CH_2)$_8$-)), 0.86-0.88 (m, 12H, 4×(-CH_3)). ^{13}C NMR (126 MHz, $CDCl_3$+CH_3OD) δ =

167.43, 166.29, 165.87, 160,05, 152.11, 152.07, 142.54, 140.67, 130.73, 129.21, 124.04, 108.93, 107.66, 106.47, 106.38, 103.56, 102.71, 79.80, 75.24, 74.76, 74.44, 73.26, 73.02, 72.19, 71.61, 71.60, 70.83, 70.40, 70.31, 70.25, 70.16, 70.12, 69.29, 69.06, 68.59, 68.41, 68.17, 64.11, 63.78, 63.32, 61.39, 61.13, 59.59, 58.65, 50.32, 31.70, 29.46, 29.42, 29.38, 29.21, 29.13, 28.97, 25.83, 22.45, 13.83. MALDI-TOF (m/z): $[M+Na]^+$ calcd for $C_{142}H_{240}N_4NaO_{48}$, 2794.3; found 2793.9.

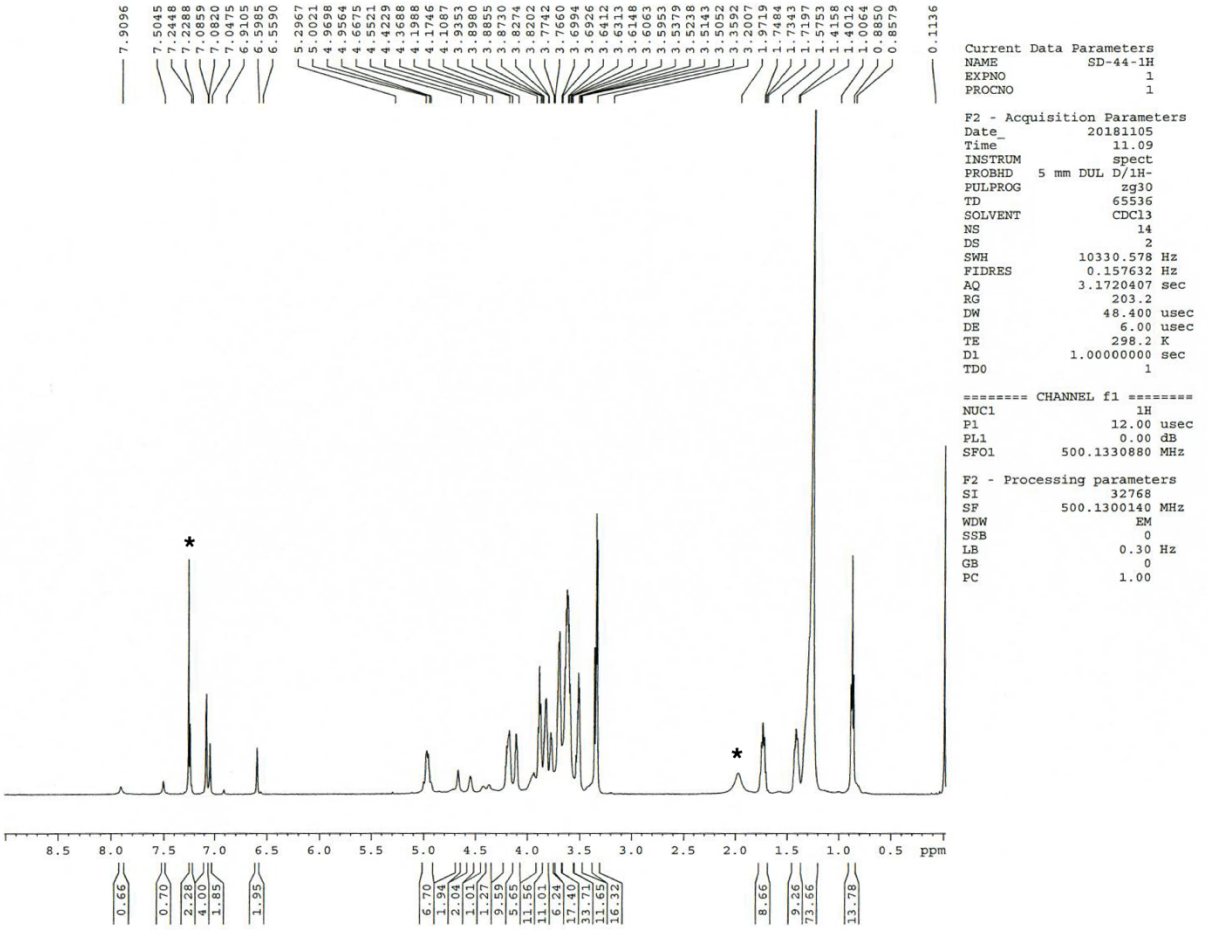

Fig. S10. The ^{1}H NMR spectrum of **JGD(5/1$_{Lac}^2$)** ($CDCl_3$, 500 MHz). Asterisked signals at δ 7.26 ppm and 1.97 ppm are due to partially nondeuterated residues of $CDCl_3$ and water, respectively.

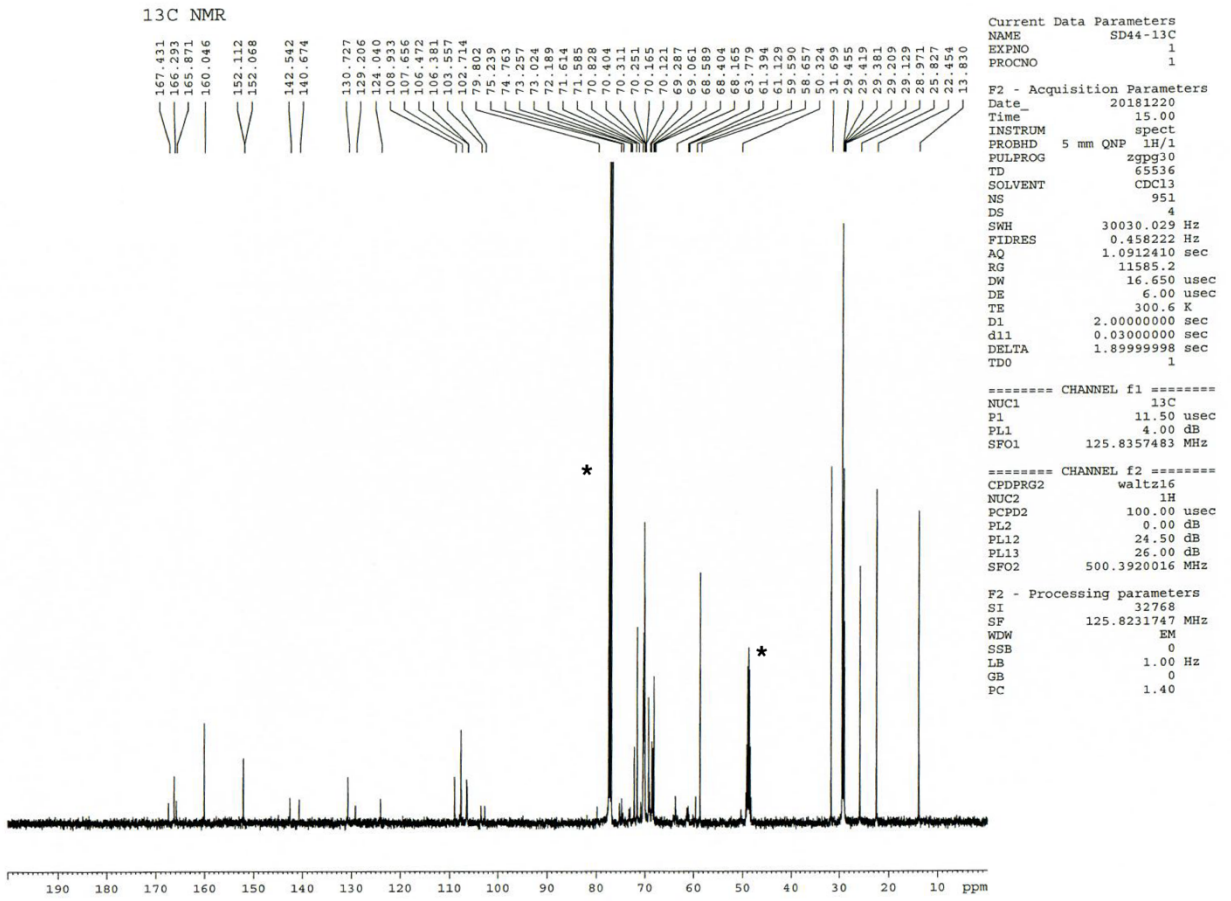

Fig. S11. The ^{13}C NMR spectrum of **JGD(5/1$_{Lac}^2$)** ($CDCl_3$+CD_3OD, 126 MHz). Asterisked signals at δ 77.16 ppm and 49.00 are due to $CDCl_3$ and CD_3OD, respectively.

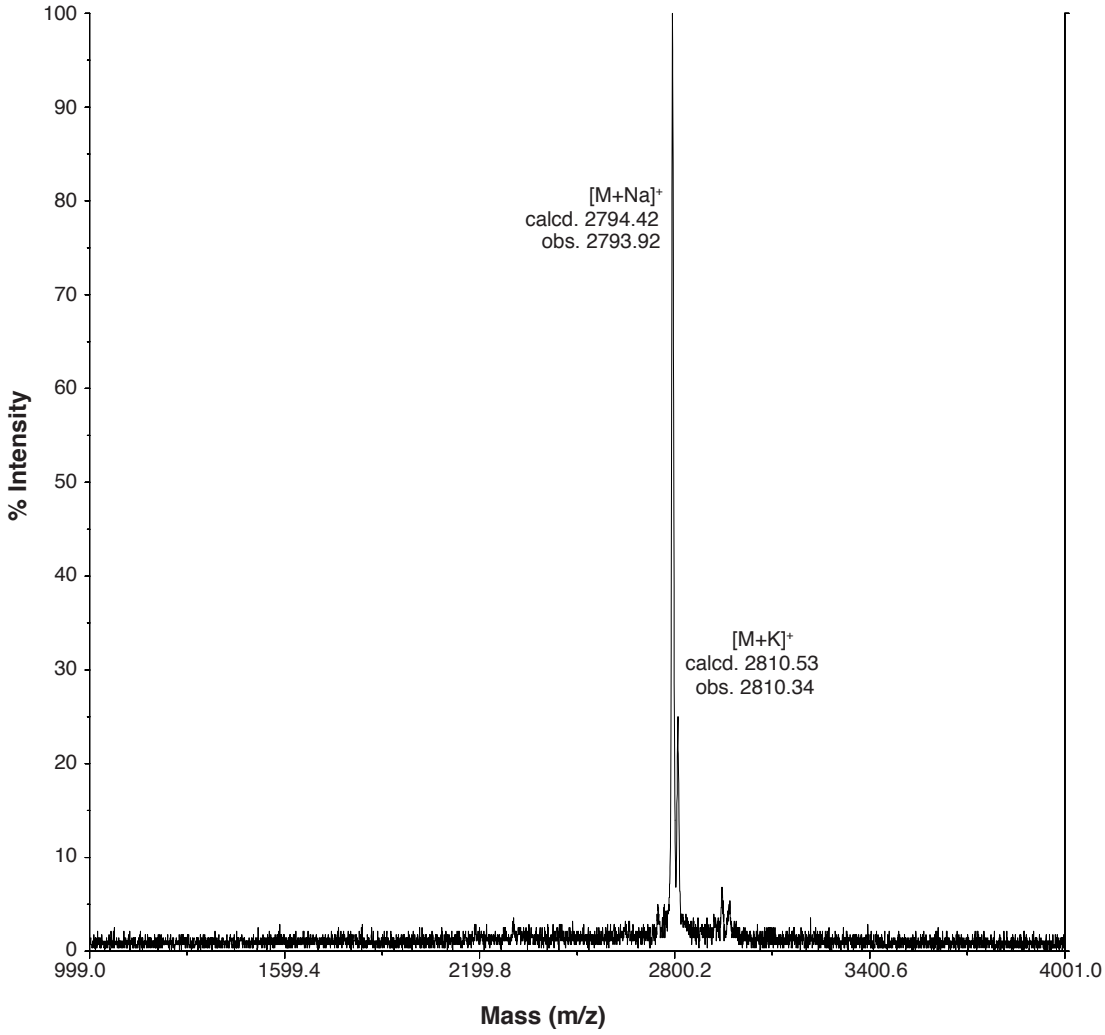

Fig. S12. MALDI-TOF mass spectrum of compound **JGD(5/1$_{Lac}^{2}$)**.

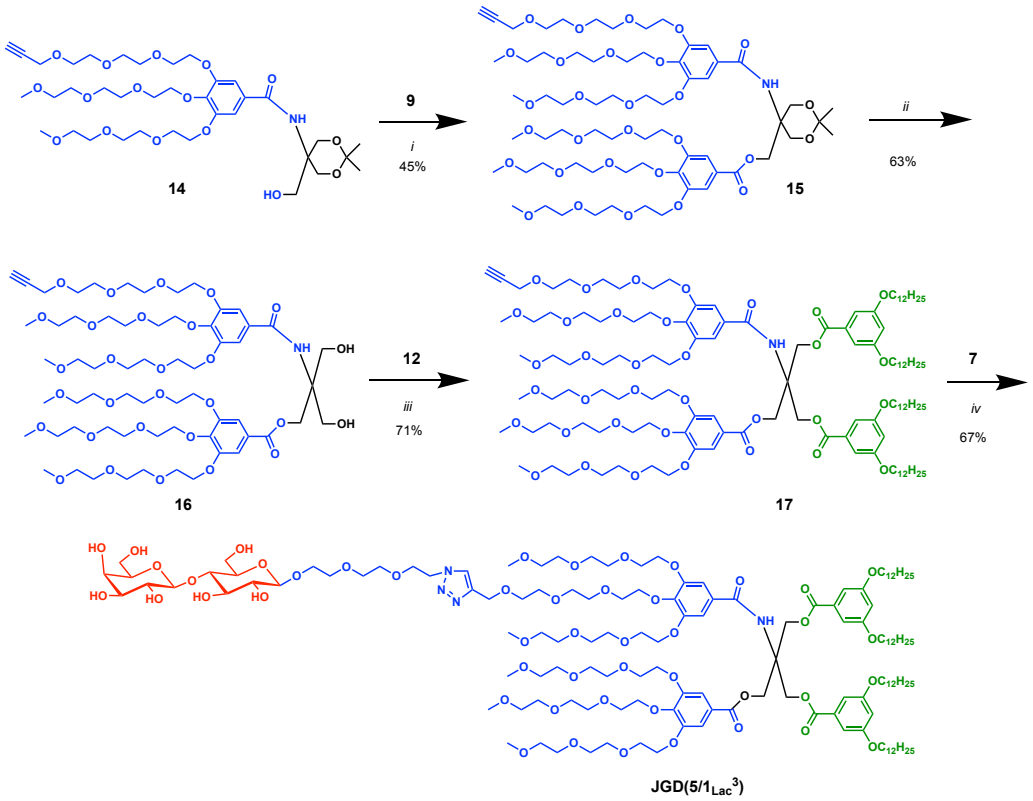

Fig. S13. Synthesis of JGD(5/1$_{Lac}^{3}$). *Reagents and conditions*: (*i*) DPTS, DCC, DCM, 23 °C; (*ii*) MeOH, HCl (2M, aq), 23 °C; (*iii*) DPTS, DCC, DCM, 23 °C; (*iv*) $CuSO_4 \cdot 5H_2O$, sodium ascorbate, THF, H_2O, 23 °C.

*Synthesis of Compound **15***. To a DCM (10 mL) solution of compound **14** (497 mg, 0.64 mmol), compound **9** (398 mg, 0.65 mmol) and DPTS (190 mg, 0.64 mmol), was added DCC (267 mg, 1.29 mmol). The mixture was allowed to stir at 23 ºC for 24 h. The precipitate was filtered, and the filtrate was concentrated to dryness. The crude product was further purified by column chromatography with a mobile phase of DCM/methanol = 40/1 (v/v) to yield compound **15** as a colorless oily liquid (394 mg, 45%). ^{1}H NMR (500 MHz, $CDCl_3$) δ = 7.30 (s, 2H, 2×Ph*H*), 7.13 (s, 1H, -N*H*), 7.04 (s, 2H, 2×Ph*H*), 4.82 (s, 2H, -COOC*H*$_2$), 4.64 (d, 2H, J = 11.9 Hz, -OC*H*$_2$), 4.15-4.23 (m, 16H, 6×(PhOC*H*$_2$CH$_2$O-) and -OC*H*$_2$CCH and -OC*H*$_2$), 3.84-3.88 (m, 12H, 6 × (PhOCH$_2$C*H*$_2$O-)), 3.69-3.72 (m, 12H, 6 × (PhOCH$_2$CH$_2$OC*H*$_2$CH$_2$O-)), 3.61-3.66 (m, 24H, 6×(PhOCH$_2$CH$_2$OCH$_2$C*H*$_2$OC*H*$_2$CH$_2$-)), 3.51-3.54 (m, 12H, 6×(PhOCH$_2$CH$_2$OCH$_2$CH$_2$OCH$_2$C*H*$_2$-)), 3.35-3.36 (m, 15H, 5×(-OC*H*$_3$)), 2.43 (t, 1H, J = 2.3Hz, -CC*H*), 1.60 (s, 3H, -OCC*H*$_3$), 1.47 (s, 3H, -OCC*H*$_3$). ^{13}C NMR (126 MHz, $CDCl_3$) δ = 167.37, 167.03, 152.46, 143.35, 141.44, 129.40, 124.05, 109.47, 106.73, 98.76, 79.68, 74.69, 72.49, 72.41, 71.94, 70.79,

70.77, 70.67, 70.54, 70.52, 70.41, 69.63, 69.10, 69.07, 68.94, 64.97, 61.59, 59.03, 58.38, 54.00, 25.32, 22.28.

*Synthesis of Compound **16**.* To a methanol solution (10 mL) of compound **15** (394 mg, 0.29 mmol), were added 1 mL of HCl aqueous solution (2M). The mixture was stirred at 23 ºC for 2 h and water was added. Then, the mixture was extracted with DCM for 3 times. An organic extract was dried over Na_2SO_4, and evaporated to dryness under reduced pressure. The crude product was further purified by column chromatography with a mobile phase of DCM/methanol = 10/1 (v/v) to yield compound **16** as a colorless viscous liquid (243 mg, 63%). ^{1}H NMR (500 MHz, $CDCl_3$) δ = 7.38 (s, 1H, -N*H*), 7.32 (s, 2H, 2×Ph*H*), 7.13 (s, 2H, 2×Ph*H*), 4.64 (m, 4H, -COOCH_2 and 2×-CH_2O*H*), 4.17-4.24 (m, 14H, 6×(-PhOC$H_2$$CH_2$O-) and -OC$H_2$CCH), 3.82-3.93 (m, 12H, 6×(PhOCH$_2$CH_2O-)), 3.75-3.79 (m, 4H, 2×(-CH_2OH)), 3.69-3.72 (m, 12H, 6 × (PhOCH$_2$CH$_2$OCH_2CH$_2$O-)), 3.61-3.67 (m, 24H, 6 × (PhOCH$_2$CH$_2$OCH$_2$CH_2OCH_2CH$_2$-)), 3.51-3.55 (m, 12H, 6×(PhOCH$_2$CH$_2$OCH$_2$CH_2OCH$_2$CH_2-)), 3.35-3.37 (m, 15H, 5×(-OCH_3)), 2.44 (t, 1H, J = 2.2Hz, -CC*H*). ^{13}C NMR (126 MHz, $CDCl_3$) δ = 168.26, 166.66, 152.42, 152.36, 143.02, 141.45, 129.33, 124.36, 109.47, 107.41, 79.61, 74.78, 72.42, 72.32, 71.94, 71.92, 71.90, 71.87, 71.82, 70.72, 70.64, 70.60, 70.54, 70.50, 70.49, 70.43, 70.38, 70.33, 69.64, 69.60, 69.08, 68.99, 63.55, 63.18, 62.03, 59.02, 58.40.

*Synthesis of Compound **17**.* To a DCM (10 mL) solution of compound **16** (187 mg, 0.14 mmol), compound **12** (140 mg, 0.28 mmol) and DPTS (85 mg, 0.29 mmol), was added DCC (120 mg, 0.58 mmol). The mixture was allowed to stir at 23 ºC for 24 h. The precipitate was filtered, and the filtrate was concentrated to dryness. The crude product was further purified by column chromatography with a mobile phase of DCM/methanol = 20/1 (v/v) to yield compound **17** as a colorless oily liquid (228 mg, 71%). ^{1}H NMR (500 MHz, $CDCl_3$) δ = 7.40 (s, 1H, -NH), 7.24 (s, 2H, 2×Ph*H*), 7.08 (d, 4H, J = 2.5Hz, 4×Ph*H*), 7.04 (s, 2H, 2×Ph*H*), 6.60 (t, 2H, J = 2.2Hz, 2×Ph*H*), 4.94-4.99 (m, 6H, 3×(-COOCH_2)), 4.10-4.21 (m, 14H, 6×(-PhOC$H_2$$CH_2$O-) and -OC$H_2$CCH), 3.89 (t, 8H, J = 6.5Hz, 4×(PhOCH_2-)), 3.82-3.85 (m, 12H, 6×(PhOCH$_2$CH_2O-)), 3.69-3.72 (m, 12H, 6 × (PhOCH$_2$CH$_2$OCH_2CH$_2$O-)), 3.60-3.66 (m, 24H, 6 × (PhOCH$_2$CH$_2$OCH$_2$CH_2OCH_2CH$_2$-)), 3.50-3.54 (m, 12H, 6×(PhOCH$_2$CH$_2$OCH$_2$CH$_2$OCH$_2$CH_2-)), 3.34-3.36 (m, 15H, 5×(-OCH_3)), 2.44 (t, 1H, J = 2.2Hz, -CCH), 1.72-1.76 (m, 8H, 4×(PhOCH$_2$CH_2-)), 1.39-1.45 (m, 8H, 4×(PhOCH$_2$CH$_2$CH_2-)), 1.26-1.32 (m, 64H, 4×(PhOCH$_2$CH$_2$CH$_2$(CH_2)$_8$-)), 0.86-0.89 (m,

12H, 4×(-C*H*$_3$)). ^{13}C NMR (126 MHz, $CDCl_3$) δ = 167.07, 166.56, 166.26, 160.30, 152.59, 152.45, 143.24, 141.50, 130.97, 129.04, 124.02, 109.29, 107.89, 106.79, 106,48, 79.75, 74.66, 72.53, 72.01, 72.00, 70.85, 70.75, 70.73, 70.61, 70.48, 69.68, 69.17, 69.00, 68.90, 68.40, 64.13, 60.07, 59.04, 58.42, 31.98, 29.75, 29.71, 29.67, 29.51, 29.42, 29.27, 26.12, 22.75, 14.18.

Synthesis of Compound ***JGD(5/1$_{Lac}^3$)***. To a mixed solution of compound **17** (101 mg, 0.04 mmol) in THF (10 mL) and **7** (24 mg, 0.05 mmol) in water (1 mL) was added $CuSO_4 \cdot 5H_2O$ (13 mg, 0.05 mmol) in water (1 mL), and sodium ascorbate (19 mg, 0.10 mmol) in water (1 mL), successively, under nitrogen atmosphere. The reaction mixture was allowed to stir at 23 °C for 24 h. The reaction mixture was concentrated to dryness. The crude product was further purified by silica column chromatography with a mobile phase of DCM/methanol = 5/1 (v/v) to yield **JGD(5/1$_{Lac}^3$)** as a colorless gel (68 mg, 67%). Purity (HPLC): 99%+. ^{1}H NMR (500 MHz, $CDCl_3$) δ = 7.92 (s, 1H, -N*H*), 7.54 (s, 1H, -CC*H*N-), 7.24 (s, 2H, 2×Ph*H*), 7.08 (s, 4H, 4×Ph*H*), 7.05 (s, 2H, 2×Ph*H*), 6.56 (s, 2H, 2×Ph*H*), 4.95-5.00 (m, 7H, 3×(-COOC*H*$_2$-) and -OC*H*O-), 4.66 (s, 2H, 2×(-O*H*)), 4.55 (s, 2H, 2×(-O*H*)), 4.35 (m, 2H, -O*H* and -OC*H*O-), 4.10-4.21 (m, 16H, 6×(-PhOC*H*$_2$CH$_2$O-) and -NC*H*$_2$C*H*$_2$O-), 3.94 (m, 2H, 2×(-CH$_2$O*H*)), 3.87-3.90 (m, 12H, 4×(PhOC*H*$_2$-) and -NCH$_2$CH$_2$OC*H*$_2$C*H*$_2$O-), 3.77-3.88 (m, 16H, 6×(PhOCH$_2$C*H*$_2$O-) and -NCH$_2$CH$_2$OCH$_2$CH$_2$OC*H*$_2$C*H*$_2$O-), 3.58-3.70 (m, 48H, 6×(PhOCH$_2$CH$_2$OC*H*$_2$C*H*$_2$OC*H*$_2$C*H*$_2$-)), 3.52 (m, 12H, 6×(PhOCH$_2$CH$_2$OCH$_2$CH$_2$OCH$_2$C*H*$_2$-)), 3.34-3.36 (m, 15H, 5×(-OC*H*$_3$)), 1.72-1.75 (m, 8H, 4×(PhOCH$_2$C*H*$_2$-)), 1.40-1.41 (m, 8H, 4×(PhOCH$_2$CH$_2$C*H*$_2$-)), 1.25 (m, 64H, 4×(PhOCH$_2$CH$_2$CH$_2$(C*H*$_2$)$_8$-)), 0.86-0.88 (m, 12H, 4×(-C*H*$_3$)). ^{13}C NMR (126 MHz, $CDCl_3$+CH_3OD) δ = 166.40, 165.89, 160.12, 152.20, 152.07, 142.37, 140.62, 130.76, 129.27, 124.23, 108.92, 107.73, 106.48, 103.60, 102.82, 79.92, 75.33, 74.82, 74.61, 73.36, 72.22, 72.17, 71.64, 71.56, 70.98, 70.39, 70.34, 70.31, 70.26, 70.18, 70.14, 69.39, 69.28, 69.15, 68.96, 68.56, 68.43, 68.25, 64.16, 63.84, 61.46, 61.16, 59.64, 58.71, 50.25, 31.77, 29.53, 29.49, 29.46, 29.29, 29.20, 29.04, 25.90, 22.52, 13.86. MALDI-TOF (m/z): $[M+Na]^+$ calcd for $C_{142}H_{240}N_4NaO_{48}$, 2794.3; found 2793.6.

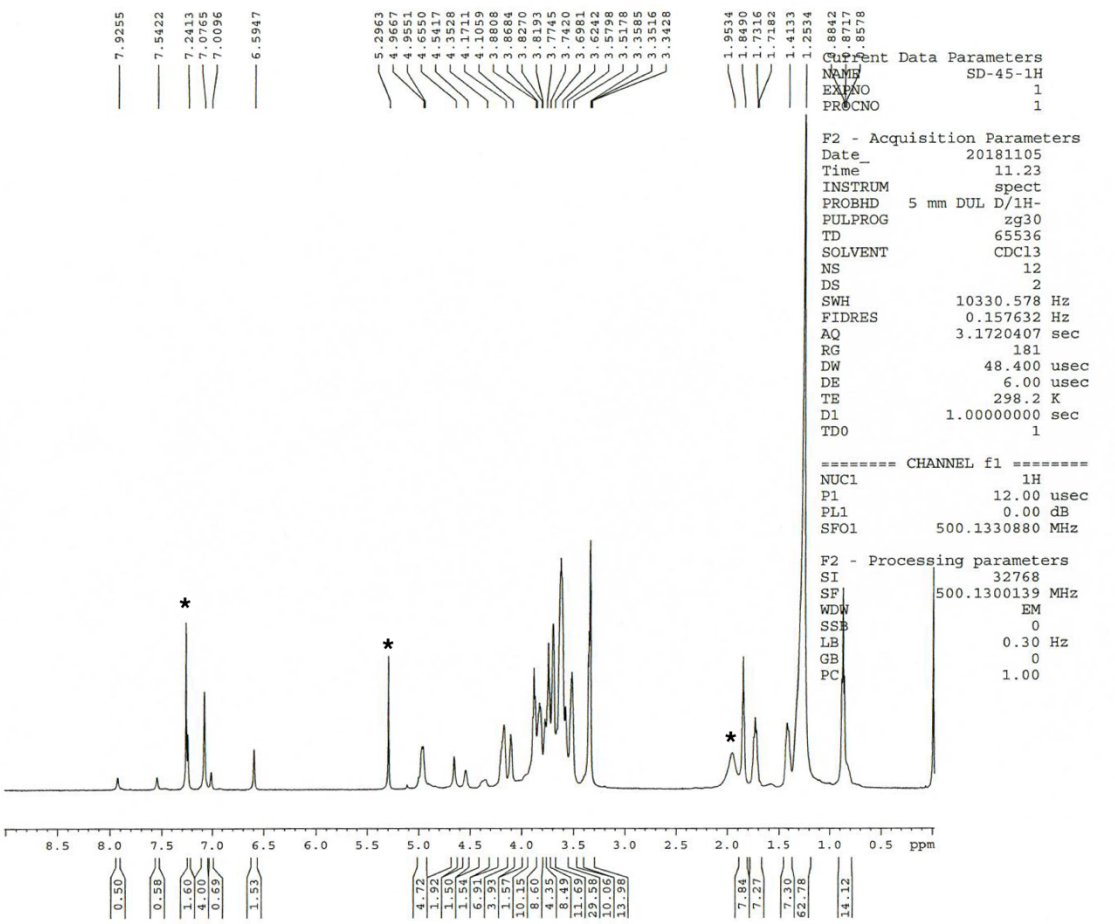

Fig. S14. The ^{1}H NMR spectrum of **JGD(5/1$_{Lac}^{3}$)** ($CDCl_3$, 500 MHz). Asterisked signals at δ 7.26 ppm, 1.97 ppm, 5.30 ppm are due to partially nondeuterated residues of $CDCl_3$ and water, and trace DCM, respectively.

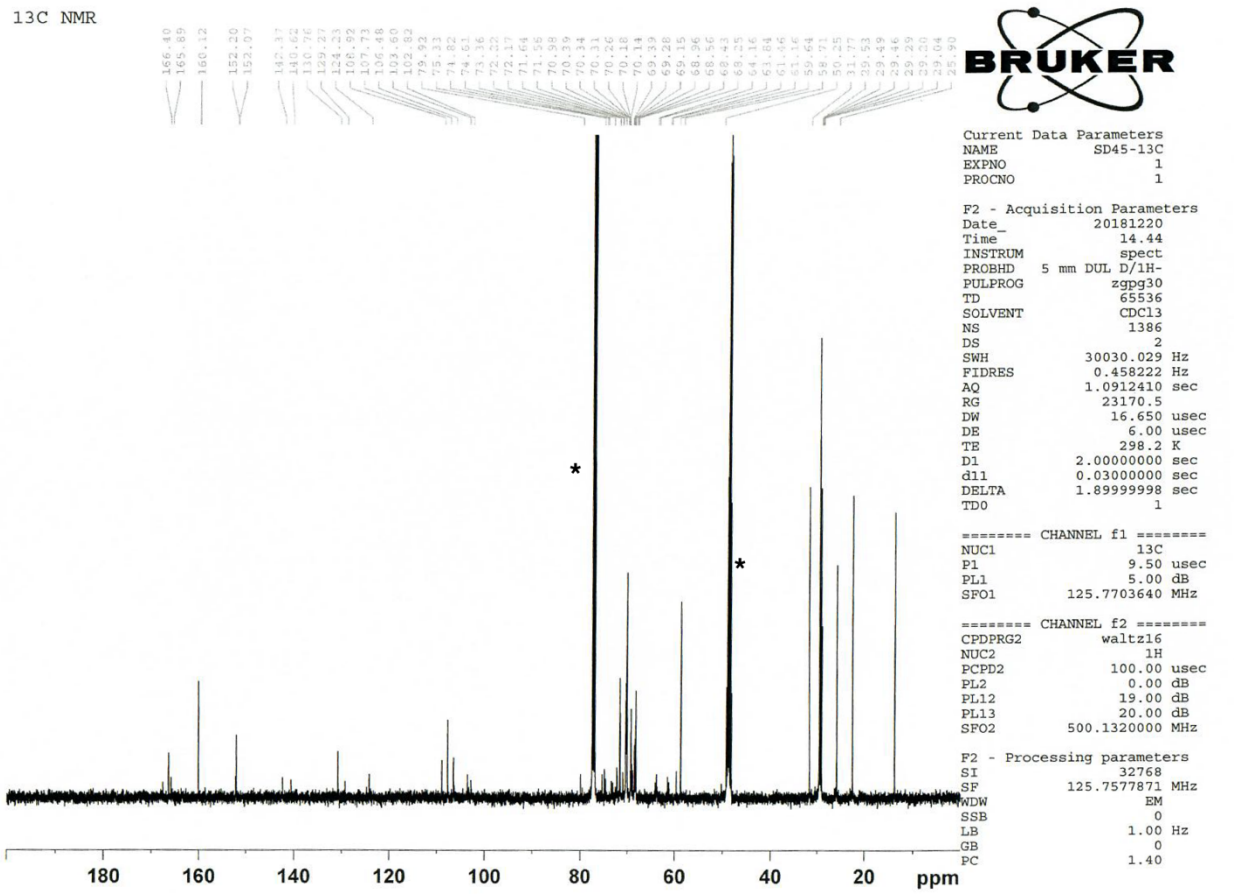

Fig. S15. The ^{13}C NMR spectrum of **JGD(5/1$_{Lac}^{3}$)** ($CDCl_3$+CD_3OD, 126 MHz). Asterisked signals at δ 77.16 ppm and 49.00 are due to $CDCl_3$ and CD_3OD, respectively.

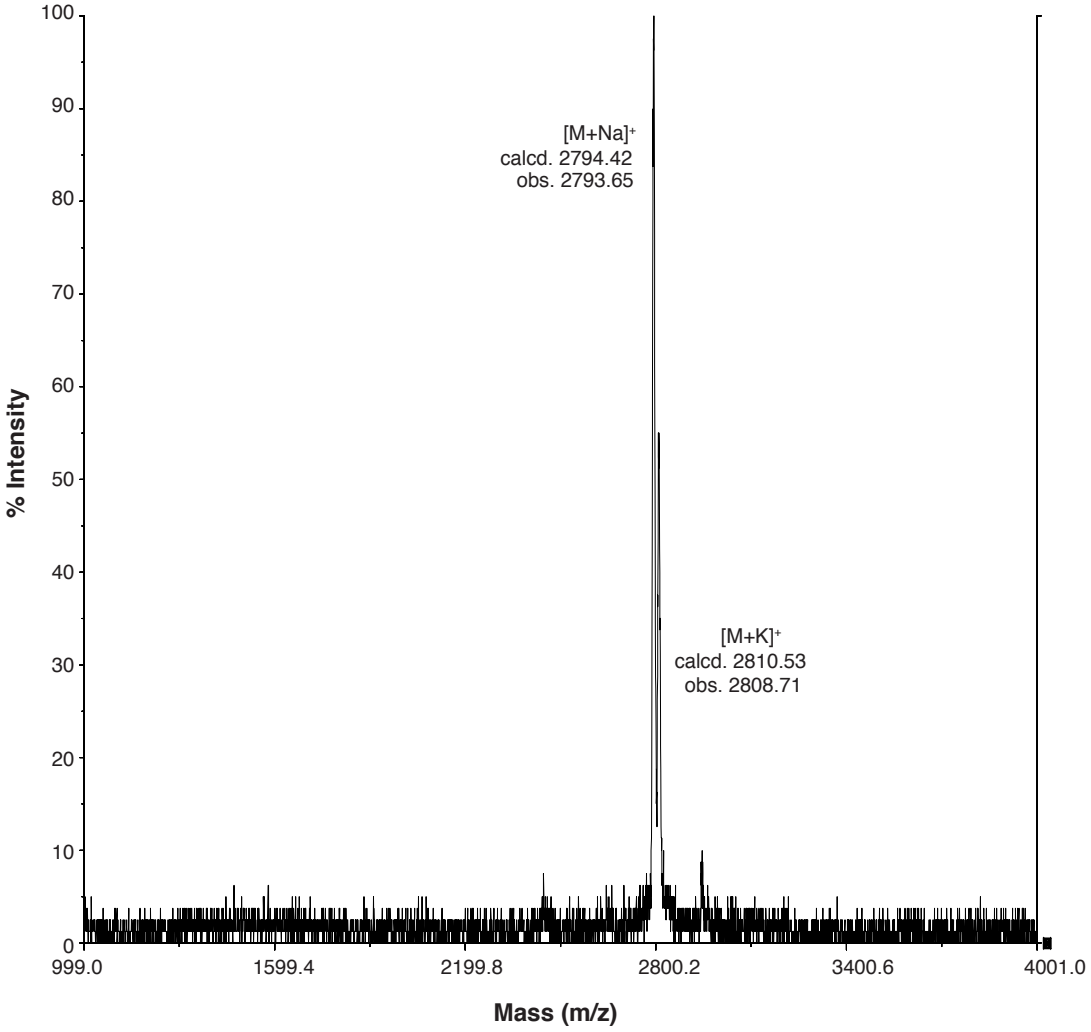

Fig. S16. MALDI-TOF mass spectrum of compound **JGD(5/1$_{Lac}^{2}$)**.

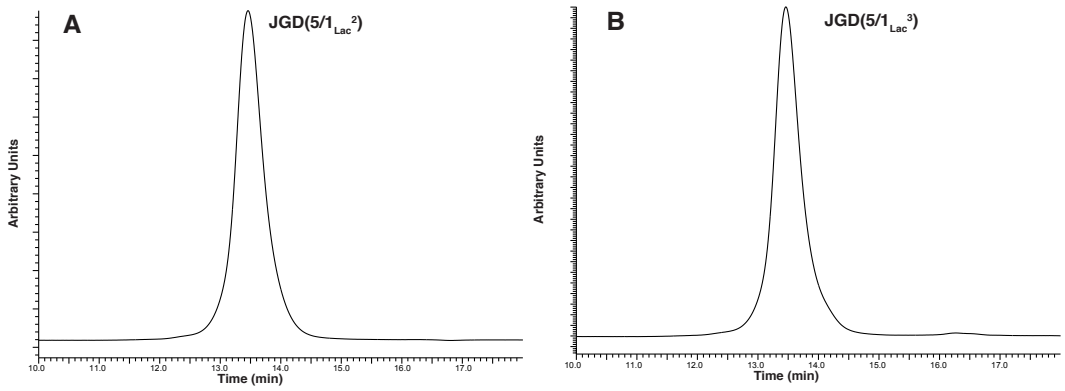

Fig. S17. HPLC traces. **A**, HPLC trace of **JGD(5/1$_{Lac}^{2}$)**; **B**, HPLC trace of **JGD(5/1$_{Lac}^{3}$)**. UV-*vis* detector was set at $\lambda = 254$ nm.

4. Aggregation Assays

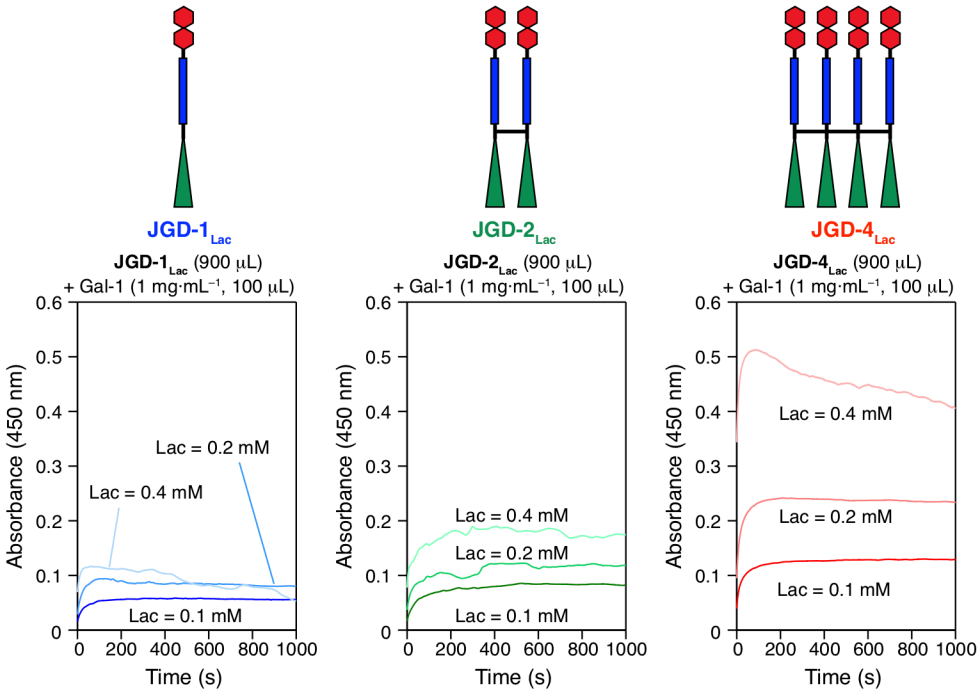

Fig. S18. Aggregation assays of GDSs. Aggregation assays of GDSs (900 μL) from self-assembly of JGDs with high density of sugar with Gal-1 (1 mg·mL^{-1}, 100 μL).

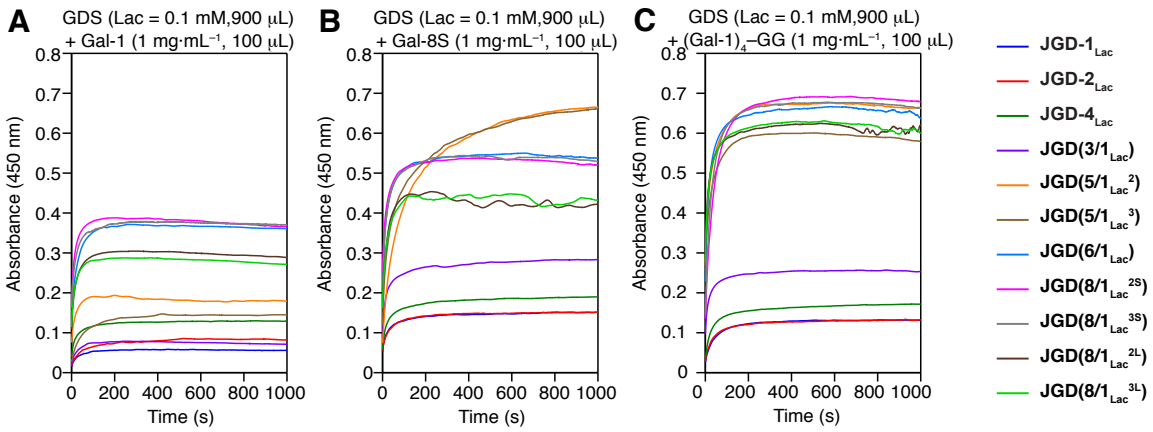

Fig. S19. Aggregation assays of sequence-defined GDSs. A–C, Aggregation assays of GDS (900 μL) from self-assembly of sequence-defined with A, Gal-1 (1 mg·mL^{-1}, 100 μL), B, Gal-8S (1 mg·mL^{-1}, 100 μL), and C, (Gal-1)$_4$–GG (1 mg·mL^{-1}, 100 μL).

5. Atomic Force Microscopy

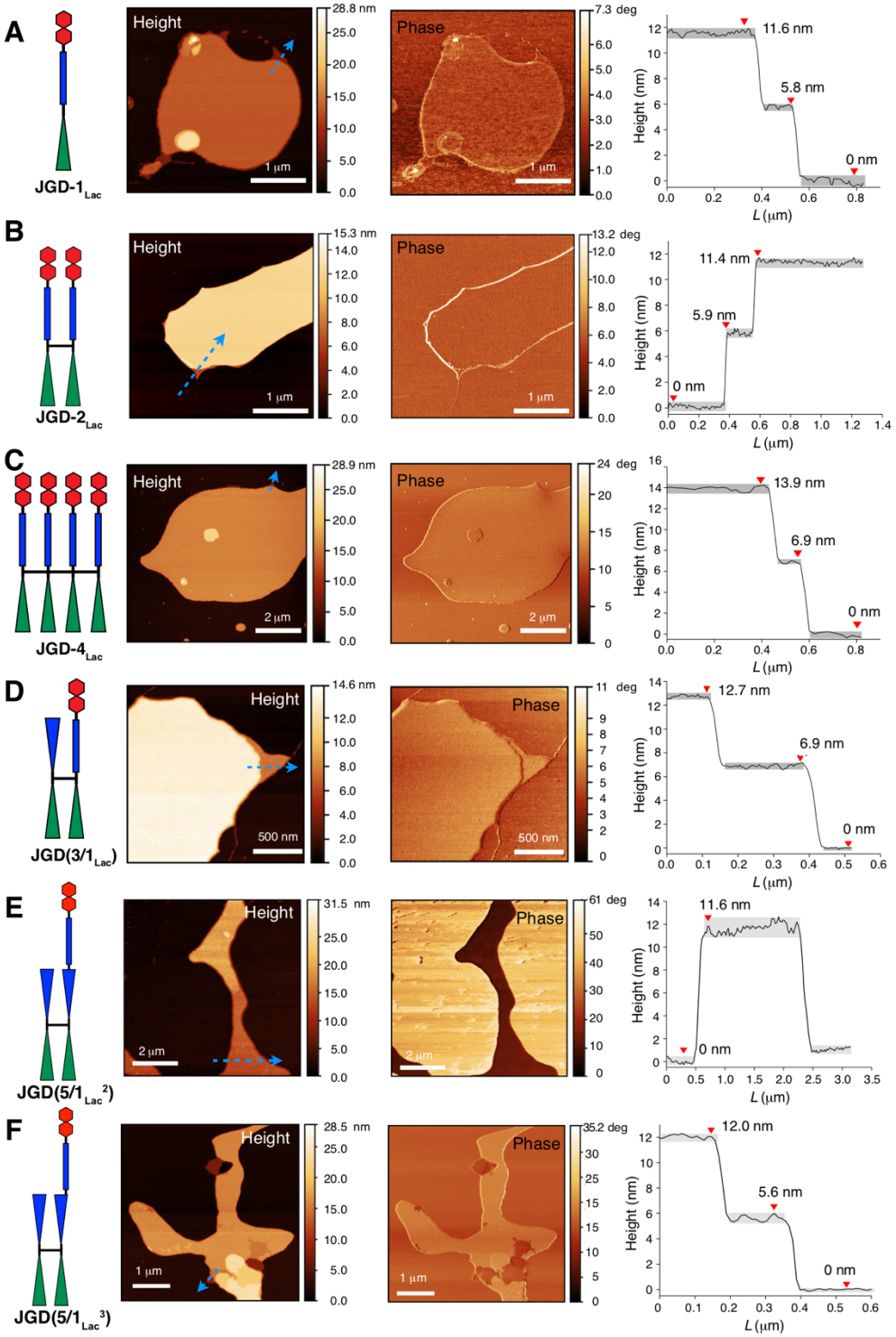

Fig. S20. Atomic force microscopy (AFM) images and the corresponding height profile of dry GDSs on mica. A, JGD-1$_{Lac}$; B, JGD-2$_{Lac}$; C, JGD-4$_{Lac}$; D, JGD(3/1$_{Lac}$); E, JGD(5/1$_{Lac}^2$); F, JGD(5/1$_{Lac}^3$)..

Blue arrow indicates the direction for analysis of the height profile. Double bilayers arise from the collapse of the 3-dimensional GDS onto a flat mica substrate.

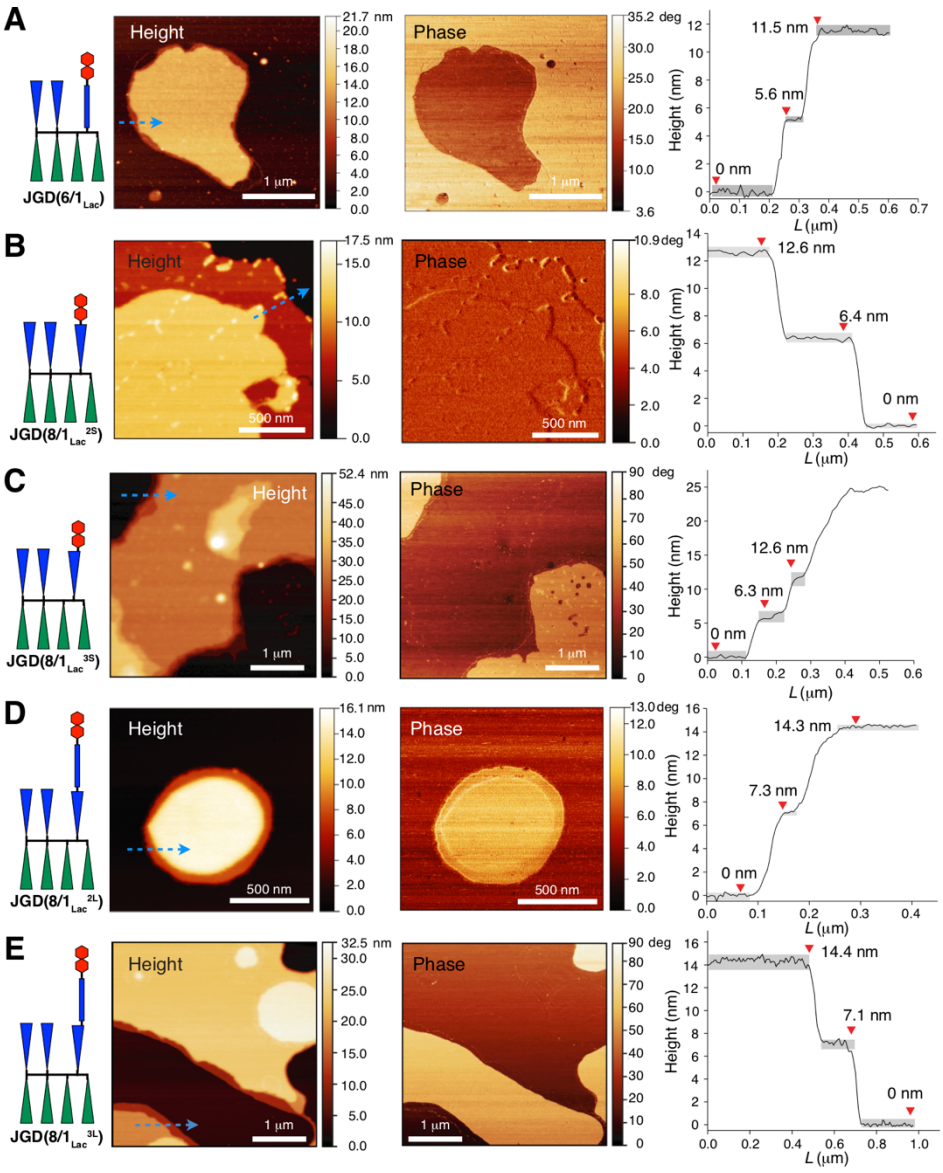

Fig. S21. AFM images of dry GDSs on mica. Height and phase images of **A, JGD(6/1$_{Lac}$)**; **B, JGD(8/1$_{Lac}^{2S}$)**; **C, JGD(8/1$_{Lac}^{3S}$)**; **D, JGD(8/1$_{Lac}^{2L}$)**; **E, JGD(8/1$_{Lac}^{3L}$)**. Blue arrows indicate the directions for analysis of the height profiles (right). For all molecules, height profiles at the edge of the dried sample show double and single bilayers. Double bilayers arise from the collapse of the 3-dimensional GDS onto a flat mica substrate.

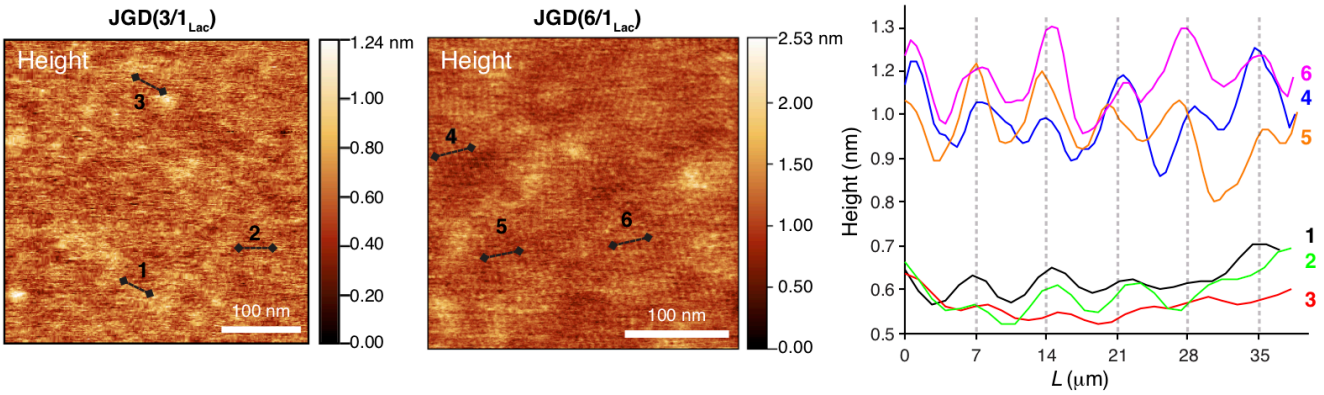

Fig. S22. AFM height images and height profile plots. Black lines numbered 1 to 6 indicate the directions for analysis of the height profiles (right). Height profiles for the lamellar structures of **JGD(3/1$_{Lac}$)** and **JGD(6/1$_{Lac}$)** show that the interlamellar spacing in both molecules is ~7 nm, but that the relative height distance between lamellar striations is much larger for **JGD(3/1$_{Lac}$)** (lines 1 to 3) than for **JGD(6/1$_{Lac}$)** (lines 4 to 6).

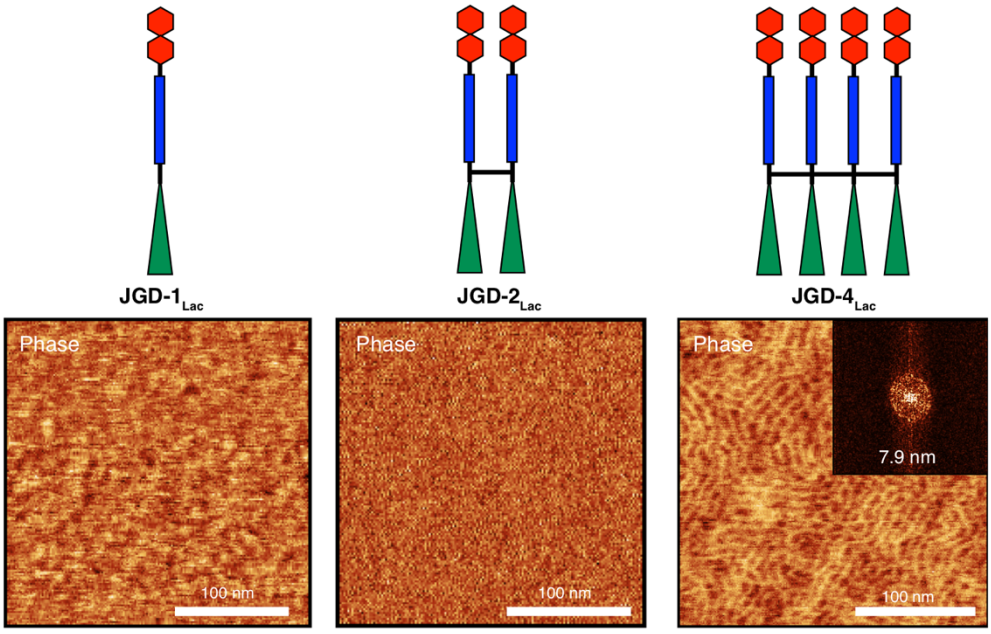

Fig. S23. AFM phase images and bilayer and vesicle models of dry GDSs on mica prepared by self-assembly of JGDs. Self-assembly of GDSs with high density sugar from **JGD-1, JGD-2**, and **JGD-4**. (Inset) Fast Fourier transform (FFT) of AFM phase images. Phase images map material differences rather than height differences. For both **JGD-1$_{Lac}$** and **JGD-2$_{Lac}$**, the phase images show a homogeneous pattern across the sample, suggesting that the surface of the GDS is also homogeneous. In contrast, lamellar striations are apparent for **JGD-4$_{Lac}$** (right), suggesting a striated pattern on the surface of the GDS. FFT of the phase image of **JGD-4$_{Lac}$** generates features with a single distance, 7.9 nm, corresponding to the average distance between adjacent lamellae on the GDS surface.

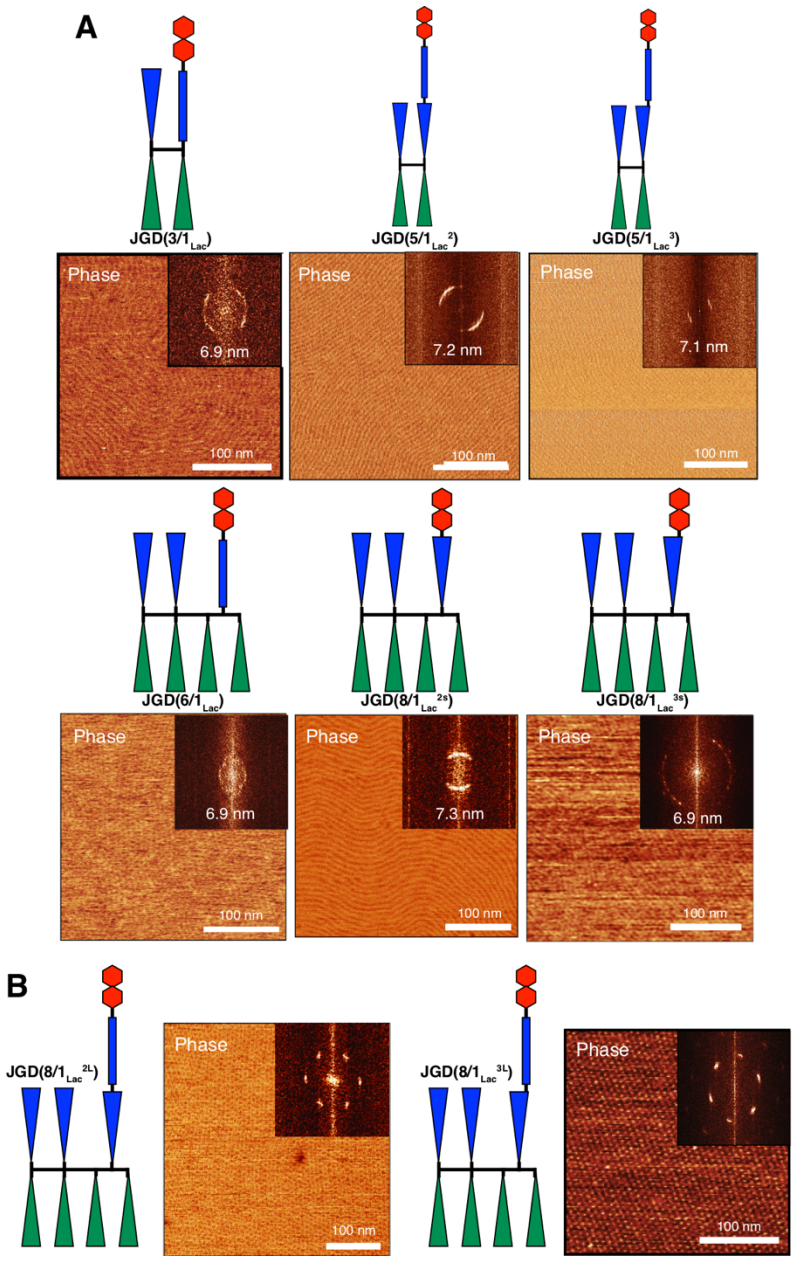

Fig. S24. AFM phase images and bilayer and vesicle models of dry GDSs on mica prepared by self-assembly of JGDs. Self-assembly of GDSs with low density sugar from **a**, **JGD(3/1$_{Lac}$)**, **JGD(6/1$_{Lac}$)**, **JGD(8/1$_{Lac}^{2S}$)**, and **JGD(8/1$_{Lac}^{3S}$)** and **b**, **JGD(8/1$_{Lac}^{2L}$)** and **JGD(8/1$_{Lac}^{3L}$)**. (Inset) Fast Fourier transform (FFT) of AFM phase images. Phase images map material differences rather than height differences. For **JGD(3/1$_{Lac}$)**, **JGD(6/1$_{Lac}$)**, **JGD(8/1$_{Lac}^{2S}$)**, and **JGD(8/1$_{Lac}^{3S}$)**, lamellar striations are observed, corresponding to a lamellar morphology on the GDS surface. Interlamellar spacing, determined by FFT, is 6.9 nm for all three molecules. The phase images of **JGD(8/1$_{Lac}^{2L}$)** and **JGD(8/1$_{Lac}^{3L}$)** show a hexagonal pattern, which is confirmed by indexing of the peaks obtained by FFT (Fig. 5C).

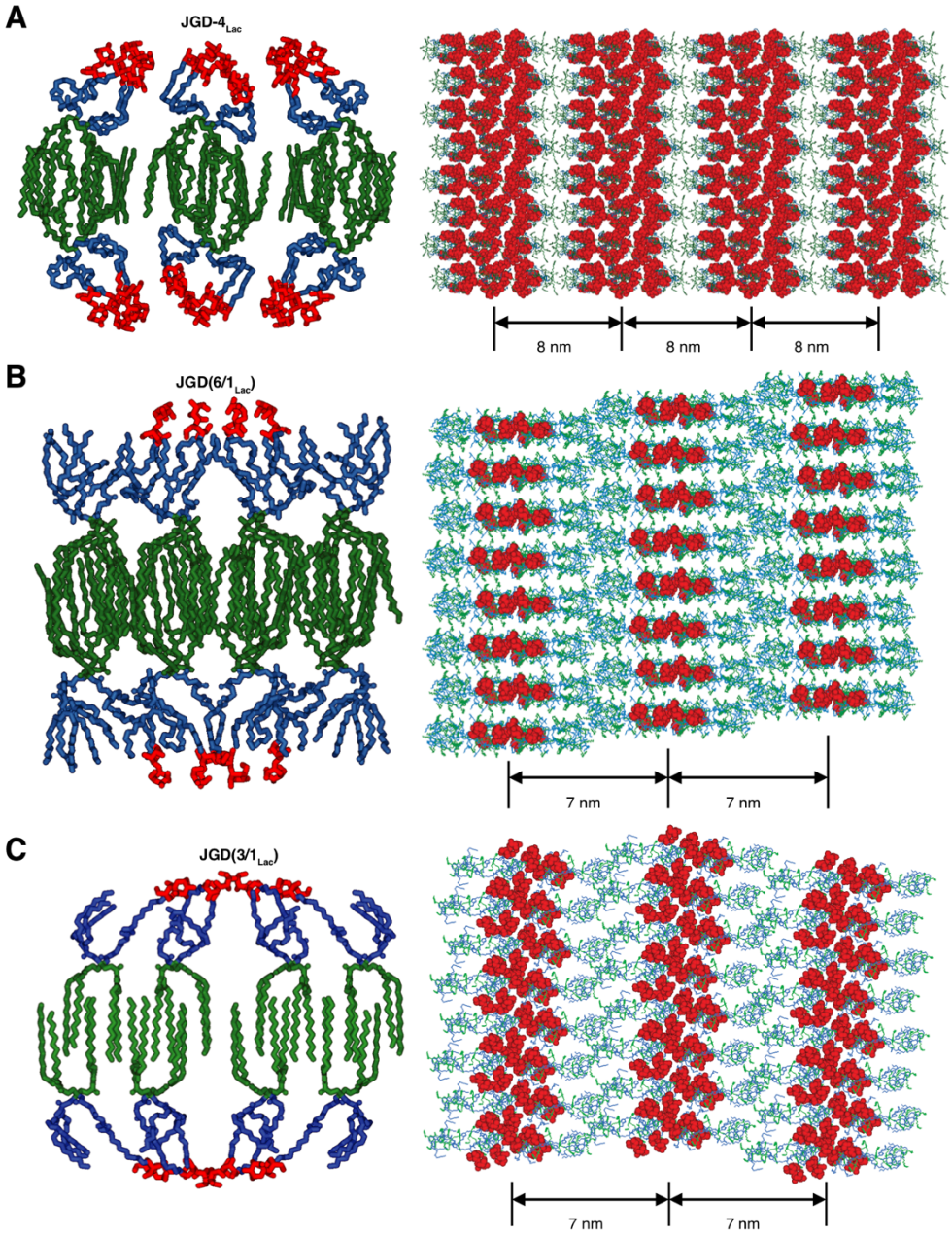

Fig. S25. Models of the bilayer structures with nanosegregation. a, **JGD-4$_{Lac}$**; **b**, **JGD(6/1$_{Lac}$)**; **c**, **JGD(3/1$_{Lac}$)**. (left) Schematic depiction of single sugar cluster (side view). Sugars are positioned to maximize hydrogen bonding interactions. The size of the sugar cluster is limited by the length of the linker connecting the sugar to the dendrimer. (right) Schematic depiction of bilayer (top view). This does not account for dynamics and disorder present in solution, but rather depicts an idealized structure consistent with phase modulations observed by AFM.

6. Statistical Analysis of Aggregation Assays

Table S1. Significant differences of the aggregation assays between JGD morphologies with different galectins. *P*-value is used to determine whether two groups of data are statistically different or not. TTEST function (students' t-test) from Microsoft™ Excel with two-tailed test was applied for statistically significant analysis of those two groups of data. Sample number $N = 3$ for each assay.

	Gal-1	Gal-8S	$(Gal\text{-}1)_4$-GG
No Morphology *vs* No Morphology			
JGD-1_{Lac} *vs* **JGD-2_{Lac}**	*	n.s.	n.s.
No Morphology vs LAM			
JGD-1_{Lac} *vs* **JGD-4_{Lac}**	***	*	*
JGD-2_{Lac} *vs* **JGD-4_{Lac}**	**	*	*
No Morphology vs LAM diluted			
JGD-1_{Lac} *vs* **JGD($3/1_{Lac}$)**	**	***	***
JGD-1_{Lac} *vs* **JGD($5/1_{Lac}^{2}$)**	***	***	***
JGD-1_{Lac} *vs* **JGD($6/1_{Lac}$)**	***	***	***
JGD-1_{Lac} *vs* **JGD($8/1_{Lac}^{2S}$)**	***	***	***
JGD-2_{Lac} *vs* **JGD($3/1_{Lac}$)**	n.s.	***	***
No Morphology *vs* HEX			
JGD-1_{Lac} *vs* **JGD($8/1_{Lac}^{2L}$)**	***	***	***
LAM *vs* LAM diluted			
JGD-4_{Lac} *vs* **JGD($3/1_{Lac}$)**	***	**	**
JGD-4_{Lac} *vs* **JGD($5/1_{Lac}^{3}$)**	n.s.	***	***
JGD-4_{Lac} *vs* **JGD($6/1_{Lac}$)**	***	***	***
LAM diluted *vs* LAM diluted			
JGD($3/1_{Lac}$) *vs* **JGD($5/1_{Lac}^{2}$)**	***	**	***
JGD($3/1_{Lac}$) *vs* **JGD($6/1_{Lac}$)**	***	***	***
JGD($6/1_{Lac}$) *vs* **JGD($8/1_{Lac}^{2S}$)**	n.s.	n.s.	n.s.
JGD($5/1_{Lac}^{2}$) *vs* **JGD($5/1_{Lac}^{3}$)**	*	n.s.	n.s.
JGD($8/1_{Lac}^{2S}$) *vs* **JGD($8/1_{Lac}^{3S}$)**	n.s.	n.s.	n.s.
HEX *vs* HEX			
JGD(8/1Lac^{2L}) *vs* **JGD(8/1Lac^{3L})**	n.s.	n.s.	n.s.
LAM *vs* HEX			
JGD-4_{Lac} *vs* **JGD($8/1_{Lac}^{3L}$)**	***	***	***
JGD-4_{Lac} *vs* **JGD($8/1_{Lac}^{2L}$)**	***	***	***
LAM diluted *vs* HEX			
JGD($8/1_{Lac}^{2S}$) *vs* **JGD($8/1_{Lac}^{2L}$)**	*	*	n.s.
JGD($8/1_{Lac}^{3S}$) *vs* **JGD($8/1_{Lac}^{3L}$)**	**	*	n.s.
JGD($5/1_{Lac}^{2}$) *vs* **JGD($8/1_{Lac}^{2L}$)**	**	*	n.s.
JGD($6/1_{Lac}$) *vs* **JGD($8/1_{Lac}^{2L}$)**	*	*	n.s.

LAM: lamellar morphology; HEX: hexagonal morphology. For significant difference: n.s. (no significant): $p > 0.05$; *: $0.01 < p < 0.05$; **: $0.001 < p < 0.01$; ***: $p < 0.001$.

7. Cryogenic Transmission Electron Microscopy

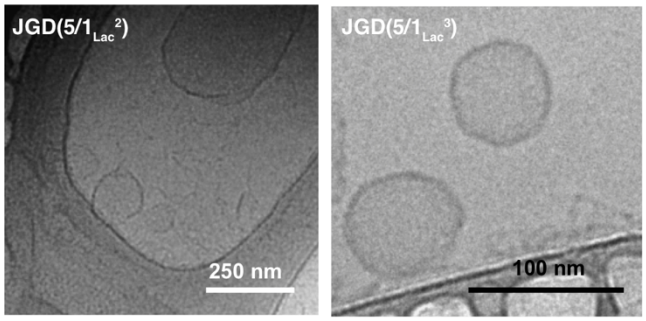

Fig. S26. Cryogenic transmission electron microscopy (Cryo-TEM) images of GDSs self-assembled by **JGD(5/1$_{Lac}^{2}$)** or **JGD(5/1$_{Lac}^{3}$)**.

5. References for the Supporting Information

1. Zhang S, et al. (2015) Dissecting molecular aspects of cell interactions using glycodendrimersomes with programmable glycan presentation and engineered human lectins. *Angew Chem Int Ed Engl* 54(13):4036–4040.
2. André S, Kaltner H, Furuike T, Nishimura S, Gabius H-J (2004) Persubstituted cyclodextrinbased glycoclusters as inhibitors of protein-carbohydrate recognition using purified plant and mammalian lectins and wild-type and lectin-gene-transfected tumor cells as targets. *Bioconjug Chem* 15:87–98
3. Kopitz J, et al. (2017) Reaction of a programmable glycan presentation of glycodendrimersomes and cells with engineered human lectins to show the sugar functionality of the cell surface. *Angew Chem Int Ed Engl* 56:14677–14681.
4. Zhang, S.; Xiao, Q.; Sherman, S. E.; Muncan, A.; Ramos Vicente, A. D. M.; Wang, Z.; Hammer, D. A.; Williams, D.; Chen, Y.; Pochan, D. J.; Vértesy, S.; André, S.; Klein, M. L.; Gabius, H.-J.; Percec, V. Glycodendrimersomes from Sequence-Defined Janus Glycodendrimers Reveal High Activity and Sensor Capacity for the Agglutination by Natural Variants of Human Lectins. *J. Am. Chem. Soc.* **2015**, *137*, 13334–13344.
5. Percec, V.; Wilson, D. A.; Leowanawat, P.; Wilson, C. J.; Hughes, A. D.; Kaucher, M. S.; Hammer, D. A.; Levine, D. H.; Kim, A. J.; Bates, F. S.; Davis, K. P.; Lodge, T. P.; Klein, M. L.; DeVane, R. H.; Aqad, E.; Rosen, B. M.; Argintaru, A. O.; Sienkowska, M. J.; Rissanen, K.; Nummelin, S.; Ropponen, J. Self-Assembly of Janus Dendrimers into Uniform Dendrimersomes and Other Complex Architectures. *Science* **2010**, *328*, 1009–1014.

6. Wu, W.; Driessen, W.; Jiang, X. Oligo(ethylene glycol)-Based Thermosensitive Dendrimers and Their Tumor Accumulation and Penetration. *J. Am. Chem. Soc.* **2014**, *136*, 3145–3155.
7. Xiao, Q.; Ludwig, A.-K.; Romano, C.; Buzzacchera, I.; Sherman, S. E.; Vetro, M.; Vertesy, S.; Kaltner, H.; Reed. E. H.; Moeller, M.; Wilson, C. J.; Hammer, D. A.; Oscarson, S.; Klein, M. L.; Gabius, H.-J.; Percec, V. Exploring Functional Pairing Between Surface Glycoconjugates and Human Galectins Using Programmable Glycodendrimersomes. *Proc. Natl. Acad. Sci. U.S.A.* **2018**, *115*, E2509–E2518.
8. Zhang, S.; Moussodia, R.-O.; Sun, H.-J.; Leowanawat, P.; Muncan, A.; Nusbaum, C. D.; Chelling, K. M.; Klein, M. L.; André, S.; Roy, R.; Gabius, H.-J.; Percec, V. Mimicking Biological Membranes with Programmable Glycan Ligands Self-Assembled from Amphiphilic Janus Glycodendrimers. *Angew. Chem. Int. Ed.* **2014**, *53*, 10899–10903.
9. Moore, J. S.; Stupp, S. I. Room Temperature Polyesterification. *Macromolecules* **1990**, *23*, 65–70.